

AN EXPERIMENTAL STUDY
OF THE
STABILITY OF A LAMINAR FLAME

Thesis by
Donald C. Curran
Lieutenant, U. S. Navy

In Partial Fulfillment of the Requirements
For the Degree of
Aeronautical Engineer

California Institute of Technology
Pasadena, California

1953

ACKNOWLEDGMENTS

The author wishes to express his appreciation to Dr. Frank E. Marble for his interest and guidance throughout the investigation.

Special thanks are given to Dr. F. H. Wright for setting up the facilities that made this investigation possible, and for his continuous day-to-day guidance and encouragement.

The author is also indebted to Mr. Clyde Stanton for his invaluable help in building and assembling the experimental equipment used.

Mrs. Elizabeth Fox's excellent work in typing the manuscript is greatly appreciated.

ABSTRACT

Knowledge of laminar flame front structure is insufficient to make exact stability calculations possible. The analysis of Landau⁽¹⁾ indicated flame front instability under all conditions. Semi-empirical corrections to Landau's result by Markstein⁽²⁾ demonstrated that a cellular flame front structure that Markstein observed experimentally might be a stable configuration. Karlovitz⁽³⁾ has proposed that there is a significant additional amount of turbulence produced in turbulent flames over that found in the upstream flow. Of particular significance is the question of whether or not a flame may take on a turbulent structure in the absence of upstream turbulence.

Therefore explorations concerning the conditions under which a laminar flame might become unstable were undertaken by burning pre-mixed propane and air using a spherical flame holder.

The resulting conical flame had annular waves develop in the flame front a short distance downstream from the flame holder. This distance decreased as fuel-air ratio was decreased and as gas mixture flow velocity increased. Lean high velocity flames showed a parallel result in the amplitude of the wave formed - the wave in this case developing to a large amplitude in a short distance with a tendency to roll up.

Another result of the investigation was that a fairly uniform wavelength of 0.27 in. was observed even though mixture, flame holder size and flow rate were varied.

The introduction of a small external turbulence source upstream of the flame front disturbed the flame - the amount of disturbance increasing with Reynolds' number of the turbulence source and with fuel-air equivalence ratio.

TABLE OF CONTENTS

| <u>PART</u> | <u>TITLE</u> | <u>PAGE</u> |
|-------------|--|-------------|
| | ACKNOWLEDGMENTS | i |
| | ABSTRACT | ii |
| | TABLE OF CONTENTS | iii |
| I | INTRODUCTION | 1 |
| II | EQUIPMENT | 3 |
| III | PROCEDURE AND PRELIMINARY EXPERIMENTS | 5 |
| IV | RESULTS AND DISCUSSION | 11 |
| | 1. Flame Front Waves | 11 |
| | 2. Regular Wavelength of the Flame Front Waves | 12 |
| | 3. Effects of Turbulent Wakes on the Flame Front | 16 |
| | REFERENCES | 19 |
| | NOMENCLATURE | 20 |
| | FIGURES | 21 |

I. INTRODUCTION

The structure of a flame can be described as either laminar or turbulent. A laminar flame front is sharply defined and smooth looking, and its position (in a flow system) is steady with time. On the other hand, a turbulent flame front's position is unsteady and the flame front zone appears thick. Turbulent burning velocities are considerably greater than laminar burning velocities.

However, knowledge of laminar flame front structure is insufficient to make exact stability calculations possible. Previous theoretical stability studies have been those of Landau⁽¹⁾ and Markstein⁽²⁾. The analysis of Landau indicated flame front instability under all conditions. The conclusion was a direct result, however, of his assumptions that the laminar flame was of infinitesimal thickness and the flame speed was independent of curvature. Experimental results of Markstein suggested that a cellular flame front structure is a stable configuration. A semi-empirical correction to Landau's result demonstrated that such a configuration is plausible.

However, if the upstream flow is highly turbulent, a turbulent flame will result. Some experimental studies of Karlovitz⁽³⁾ indicated that the turbulent burning speed cannot be accounted for by known turbulence of the upstream flow. Therefore Karlovitz proposed that a significant additional amount of turbulence is produced in the flame. The question then arises as to whether or not the turbulence is primarily associated with the flame itself and generated through flame instability. Of particular significance is the possibility that a flame may take on a turbulent structure in the absence of any upstream turbulence. The purpose of this investigation was to make

visual explorations to determine whether conditions exist under which a laminar flame might become unstable.

The flame study was made with premixed propane and air burning at atmospheric pressure. The visual information was obtained from shadowgraph and schlieren pictures of the flame. The burner used in carrying out the experiment was designed by Dr. F. H. Wright of the Jet Propulsion Laboratory, California Institute of Technology, and the facilities of this laboratory were used throughout the investigation.

II. EQUIPMENT

Observations were made on a conically-shaped flame stabilized on a single spherical flame holder in the center of a vertical gas jet. The results were recorded by taking instantaneous spark shadowgraph pictures and high speed motion pictures using the schlieren technique.

A schematic diagram of the complete burner apparatus is shown in Figure 1. The air was obtained from an electrically driven 500 cubic feet per minute centrifugal blower which maintained a 50 cubic foot settling tank at a pressure of 28 inches of water. A large throttling valve controlled the flow of air to the burner. A diffuser, calming chamber and a nozzle converging to a diameter of 2.969 inches (see Figure 2) were used to obtain a uniform velocity gas flow at the burner with as low a turbulence level as possible.

The propane was supplied to the burner from a standard 100 lb. capacity commercial propane bottle. Fuel flow was controlled by two throttling valves, and volume flow rate was measured by a No. 4 size Fischer and Porter Flowrator used in conjunction with a pressure gauge and thermocouple to measure fuel temperature and line pressure. The fuel was injected into the air line 9 feet upstream of the diffuser section.

The air velocity and volume flow rate were obtained by hot wire anemometer measurements at the 2.969 inch diameter orifice.

Instantaneous pictures of the flame front were taken with a shadowgraph system. The shadowgraph system consisted of a Liebessart spark gap used as an intense point source of light mounted

6 feet horizontally away from the flame and a photographic film mounted 6 feet from the flame on the opposite side. The film was 5 in. by 7 in. Super-XX and was mounted in a K21 aircraft camera from which the optical system had been removed so that only the rear section containing the film roll and focal plane shutter remained. The camera was powered by a 28 volt DC electrical system which advanced the film and actuated the focal plane shutter and spark gap. Pictures could be taken at five-second intervals.

High speed schlieren motion pictures of the flame were taken with a 16 mm. Fastax camera operating at speeds as high as 2800 frames per second.

III. PROCEDURE AND PRELIMINARY EXPERIMENTS

Since the purpose of the investigation was a stability study of a laminar flame, the first objective was to produce a satisfactory laminar flame. A spherical flame holder suspended on a fine nichrome wire (see Figure 3) produced a conical flame that could be easily studied using schlieren and shadowgraph techniques. This type of flame holder caused only a small disturbance to the flow of the gas mixture and avoided end effects present in two-dimensional studies.

The upstream velocity conditions were investigated by traversing the diameter of the 2.969 in. orifice with a hot wire anemometer located 1 mm. above the orifice. Figure 4 shows the results of this survey at an average velocity of 40.5 ft/sec. The flow had a maximum variation of 2% from mean stream velocity at a radius r less than 1.46 in. Closer to the edge of the jet (r greater than 1.46 in.) the velocity dropped off rapidly, and therefore the edge of the boundary-layer edge was assumed to be at approximately $r = 1.46$ in. Since the inside radius of the orifice was 1.484 in., the boundary-layer thickness was about 0.03 in.

Air flow rate was obtained by making use of the velocity profile across the 2.969 in. orifice. To compute the mean velocity

$\bar{U} = \frac{\text{volume flow}}{\text{orifice area}}$, the following formula was used:

$$\bar{U} = \frac{2\pi \int_0^R U r \, dr}{\pi R^2} = \frac{2 \int_0^R U r \, dr}{R^2}$$

(where $R = \text{orifice radius} = 1.484$ in.)

A velocity survey (Figure 4) at one air flow setting yielded 40.5 ft/sec for the value of the preceding integral, while the velocity on the duct axis was 39.7 ft/sec. Therefore $\frac{\bar{U}}{U_{axial}} = \frac{40.5}{39.7} = 1.02$. It was assumed that the velocity profile at lower speeds (down to 7 ft/sec) was sufficiently similar so that the approximation that $\frac{\bar{U}}{U_{axial}} = 1.02$ held. Therefore volume flow rate of the air (before propane was turned on) was obtained with a single measurement of axial velocity with the hot wire or pitot-static tube using the relation:

$$\begin{aligned} \text{Volume flow air} &= U_{axial} \times \frac{\bar{U}}{U_{axial}} \times \text{orifice area} \\ &= U_{axial} \text{ (ft/sec)} \times 1.02 \times 0.04806 \text{ (ft}^3\text{)} \\ &\quad \times \frac{\text{barometer (cm Hg)}}{76} \times \frac{530}{\text{Temp(R)}} \times 28317 \text{ cc/ft}^3 \\ &= 9690 \frac{U_{axial} \times \text{baro}}{\text{Temp}} \end{aligned}$$

This reduced the volume flow to standard conditions of temperature and pressure of 76 cm of mercury and 70° F, the conditions at which the calibration curves of the fuel Flowrator were given. The temperature was measured with a mercury thermometer placed in the flow stream and the pressure was assumed to be atmospheric and was measured with a barometer.

The static pressure in the 50 cu. ft. settling chamber was always greater than 28 inches of water while the static pressure in the air line at the point where the fuel was injected was never more than 0.4 inches of water for any of the air and fuel flow rates used. Therefore the air flow rate was governed almost entirely by the

pressure drop across the air throttling valve and remained essentially constant whether fuel was being injected or not. For this reason the velocity of the gas mixture at the flame holder was a function of the air rate and the fuel-air volume ratio, and could be determined by the relation:

$$\begin{aligned} U_o &= \frac{\text{Vol rate mixture}}{\text{cross section area}} = \frac{\text{Vol rate air} + \text{Vol rate propane}}{\text{area}} \\ &= \frac{\text{Vol rate air}}{\text{area}} \left(1 + \frac{\text{Vol rate propane}}{\text{Vol rate air}} \right) \\ &= \bar{U} \left(1 + \frac{\text{propane}}{\text{air}} \text{ volume ratio} \right) \end{aligned}$$

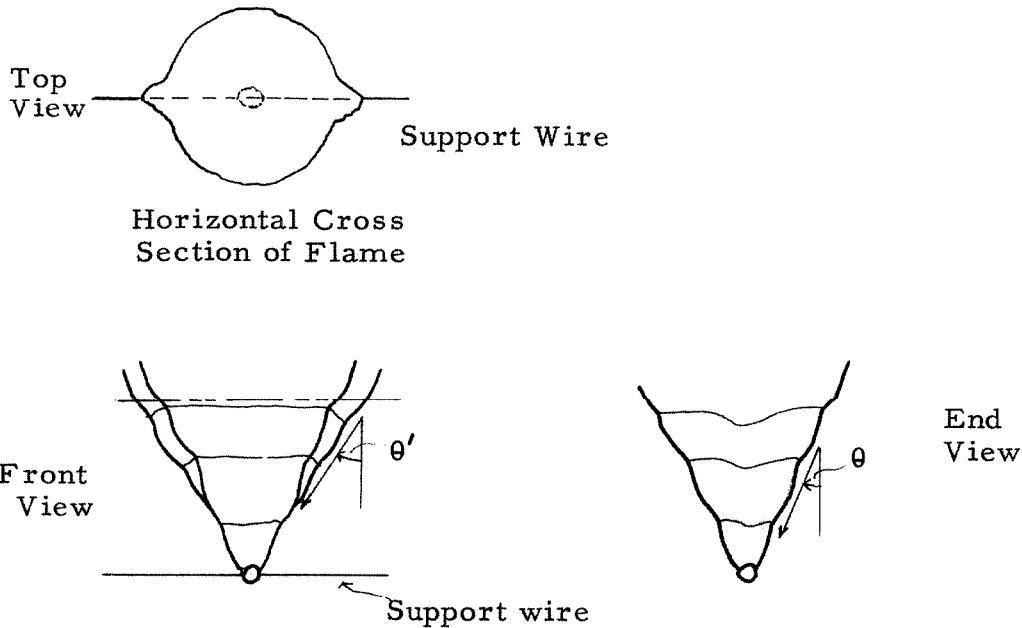
As soon as satisfactory techniques for measuring gas flow velocity U_o and equivalence ratio ϕ ($= \frac{\text{propane}}{\text{air}} \text{ volume ratio} \times \frac{1}{23.8}$) had been developed, some preliminary shadowgraphs and schlieren motion pictures of the flame were taken using various mixtures, flow velocities and flame holder diameters.

An undesirable disturbance due to periodic shedding of ring shaped vortices around the periphery of the 2.969 in. nozzle was observed in the high speed movies. This was eliminated by installing the flame in a rectangular duct with 0.25 in. thick Vycor glass walls on two opposite sides. An adapter was used that fitted on top of the 2.969 in. nozzle (see Figure 2) and reduced the cross section to a rectangular shape of 2.185 in. by 2.195 in. This rectangular cross section was maintained for 3 inches above the location of the flame holder before venting to the atmosphere. The glass walls of the duct were not optically flat, and this resulted in lines across the shadowgraph pictures of the ducted flame. However, these lines were not considered sufficiently serious to prevent proper interpretation of

the photographs.

After the rectangular duct was installed a stream turbulence survey was made. A hot wire, sensitive to small velocity fluctuations, was inserted into the gas stream close to the flame holder both with and without the flame burning. Its response to velocity fluctuations was displayed on an oscilloscope and a number of single sweep photographs (see Figure 5) of the viewplate were obtained with a 4 in. by 5 in. Speed Graphic camera. A turbulence level $\sqrt{\frac{u^2}{U}}$ of less than 0.02% at U equal 39.0 ft/sec was found and this was considered acceptable. Also no regular frequencies in the range 800 - 1400 cycles were present as can be seen in the photographs by comparing the turbulence record with the 1200 cycle calibrating signal superimposed as a second exposure on the photograph. The fairly low level of turbulence, the thin boundary layer and the nearly uniform velocity profile were indications of satisfactory upstream flow conditions in the unburned gas mixture.

Although the upstream flow conditions were satisfactory, two disturbing effects on the flame due to the flame holder support wire were observed, even though in most cases it was only 0.005 in. diameter. The support wire caused the flame to be asymmetrical when gas flow velocity was low and flame propagation velocity S_u was high (when ϕ was near 1). Three views of a slightly lean flame at U_0 about 17 ft/sec with annular wave development (to be discussed in Section IV) are sketched below:



It can be seen that $\theta' > \theta$. At very low values of U_o (around 7 ft/sec) and for ϕ near 1, θ' became considerably greater than θ (see Figures 6 and 7) and its value was very sensitive to changes in mixture ratio and velocity. When the Reynolds number Re based on the diameter of the support wire was in the range of 45 to 162, a regular short interval zig-zag pattern could be seen in the part of the flame front situated in the wake of the support wire (see Figures 8 to 12). This was presumed to be caused by a stable vortex street being shed by the latter (Reference 4). To avoid these support wire effects, the shadowgraph pictures were taken of the end view of the flame (support wire parallel to line of sight) and only the right and left edges of the flame front were studied.

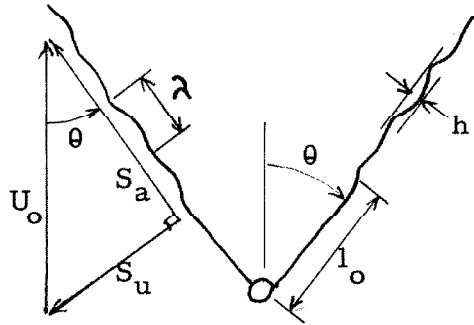
The procedure for the final experiments upon which most of the results were based was as follows: Shadowgraph pictures were taken of the ducted flame with the flame holder support wire parallel to the line of sight. The region of flame investigated was from the flame holder to a distance of 2.8 inches above it. U_o was varied between

7 and 35 ft/sec and ϕ was varied between 0.57 and 1.53. Three different spherical flame holder sizes were used - a 0.125 in., 0.25 in. and a 0.5 in. diameter. Also in one phase of the final experiments on flame front stability an outside disturbance was introduced into the flame front in the form of a turbulent wake from a small cylinder with axis vertical and supported on a 0.016 in. wire (see Figure 13). Two different sizes of cylinders were used. As another variation, a 0.095 in. diameter rod with axis perpendicular to the flow and off to one side of the flame holder was used as a turbulence source.

IV. RESULTS AND DISCUSSION

1. Flame Front Waves

At a short distance from the flame holder, the conical flame developed annular waves that propagated along the flame front at a velocity $S_a = U_o \cos \theta$ (see Figure 14 and note that all spark shadow-graphs are twice actual size).



This relation was verified from the high speed motion pictures. The wave was not noticeable until a finite distance l_o from the flame holder, usually greater than 0.3 in. The distance l_o was found to be independent of flame holder size for constant ϕ and S_a (see Figure 15). If ϕ was held constant, l_o was found to decrease with increasing S_a (see Figures 16 and 17) up to a value of about 14 ft/sec and then remained essentially constant (see Figure 18). On the other hand, if S_a was held constant, l_o increased with increasing equivalence ratio ϕ (see Figures 17 and 19) up to a value of about $\phi = 1.1$. For ϕ greater than 1.1 there were indications that l_o may have started to decrease (see Figure 20). The distance where the characteristic wave was first noticeable was a qualitative measure of the stability of the original

smooth conical flame front. As Figures 18 and 20 show, the flame with small S_a and slightly rich equivalence ratio had the most stable laminar flame front configuration since it had the greatest value of l_o .

A parallel result was observed in studying the amplitude development of the waves. Amplitude development was greater for a given distance with smaller values of equivalence ratio ϕ . (Compare Figures 21, 22 and 23). As an example, histograms of wave amplitude h vs distance l_o based on data obtained from a group of pictures similar to those of Figures 21 and 23 are shown in Figure 24. For very low values of ϕ (less than .75) the flame front wave had a tendency to become unstable and roll up about 2 inches distant from the flame holder as shown in Figures 3, 9, 11 and 12. Waves in flames with ϕ greater than .75 did not have this tendency - at least not within the distance under investigation (less than 2.8 inches above the flame holder).

2. Regular Wavelength of the Flame Front Waves

One of the most significant results of this investigation was that a uniform wavelength for the annular flame front wave was established in the region of flame under study. Based on 605 observations of various equivalence ratios, flame holder diameters, and flow velocities between 13.7 ft/sec and 28.4 ft/sec where the waves were large enough to be clearly seen, a mean wavelength $\bar{\lambda}$ of 0.27 in. was obtained.

A number of pictures were taken of each configuration of the flame, and wavelength λ vs distance l along the flame front was

measured. These wavelengths were grouped according to the distance from the flameholder (in 0.5 in. increments) at which they were observed. No definite change of λ was noted except for lean mixtures which showed an increase in λ at a distance 1 from the flameholder of about 2.0 in. (This was the same place where the lean flame front waves had a tendency to roll up.) Two examples of histograms of λ vs. 1 based on a number of pictures similar to those of Figures 21 and 23 are shown in Figure 24. The increase in λ with increasing 1 can be noted for the lean flame ($\phi = 0.79$) and the uniformity of λ can be observed for the slightly rich flame ($\phi = 1.09$).

Statistical tests applied to the mean values and deviations from the mean of the wavelengths of the above incremental distance groups showed them to be similar. Further application of the statistical tests to groups of waves from flames with different mixture ratios, flameholder sizes and velocities showed that the diverse groups were also similar. Hence, so far as can be deduced from these data, the observed waves were generated by a common mechanism, and the variability in the individual values of wavelength was due to normal scatter. The results of this statistical analysis showed the mean wavelength $\bar{\lambda}$ to be 0.2663 in., the estimated error in the mean to be 0.0040 in., the estimate s of the standard deviation to be 0.0974 in., and the estimated error in s to be 0.0028 in. A histogram summarizing these results is shown in Figure 25 and a good similarity to a normal distribution curve can be seen except for a little skewness toward the longer wavelengths.

From observations of wave frequency and propagation rate in sample sections of the high speed motion pictures, values of λ

were obtained that were close to the value of λ obtained from the shadowgraph pictures. For example: For flow velocity $U_o = 16$ ft/sec, equivalence ratio $\phi = 0.79$ and flame holder diameter = 0.5 in., was found to be 0.223 in. (which is close to $\bar{\lambda}$, varying only by 0.44 of a standard deviation found previously). For $U_o = 16$ ft/sec, $\phi = 0.79$, and a 0.125 in. diameter flame holder, λ was found to be 0.237 in. (only 0.30 of s from $\bar{\lambda}$).

In summary, the following facts about the annular flame front waves can be demonstrated by representative pictures:

(a) The wavelength did not appreciably change with equivalence ratio except for very lean mixtures (see Figures 21, 22 and 23).

(b) The wavelength did not appreciably change with gas flow velocity (see Figures 17 and 22).

(c) The wavelength did not appreciably change with spherical flame holder size (see Figures 22, 26 and 27).

The annular flame front wave has been described in detail because it was the most noticeable single phenomenon observed in the range of conditions investigated. This held promise of yielding information on the stability characteristics of the flame if it could be shown that the wave originated in the flame itself and was not caused by an external disturbance. It is well known that strong external disturbances can force oscillations in a flame front. A very likely source of external disturbance was the flame holder. However, observed results showed the wavelength λ and frequency n to be independent of flame holder size. With λ constant, $n = \frac{U_o \cos \theta}{\lambda} = n(U_o, \phi)$, since $\theta = \theta(U_o, \phi)$. On the other hand, for cold flow around bluff bodies there is a definite relation between Strouhal number $\frac{nd}{U_o}$ and

Reynolds number $\frac{U_o d}{\nu}$. From this relation it can be seen that $n = n(U_o, d, \nu)$. Also, boundary layer characteristics depend on body size. Since the observed frequency of the annular wave was independent of d it appeared that the annular waves were not directly caused by the flame holder.

A second possible external source of the flame front oscillations was upstream flow velocity fluctuation. To eliminate this possibility a careful survey with a hot wire anemometer was made of the upstream flow. No regular velocity fluctuations were found in the frequency range of the flame front wave oscillations (400 - 1500 cycles/sec). The observed fluctuations were relatively random and fell chiefly between 30 and 100 cycles/sec. Therefore it was assumed that there were no upstream flow effects generating the observed wave.

Since the most probable causes of external disturbance to the flame front had been eliminated, it appeared that the stable wave configuration observed was due to the flame itself.

Stable waves have also been found in other investigations. For example, Markstein (Ref. 2) found a cellular structure in a plane flame propagating in a tube. Although the diameters of Markstein's cells were of the same order of magnitude as the wavelengths of the waves in the conical flame, the different geometries of the two experiments made comparison difficult. There was one important difference in the results, though. Markstein found cellular waves only for rich mixtures while waves were observed for all fuel-air ratios in the conical flame. Because of these differences it was impossible

to say that the annular waves had a common origin with Markstein's cells. Both experiments did show, however, that stable wave configurations were possible for a flame front.

3. Effects of Turbulent Wakes on the Flame Front

The truly conical flame became unstable above $U_0 = 10$ ft/sec. Between 10 and 35 ft/sec (the upper observed velocity limit) the annular wave state, another stable flame front configuration, was observed. To test further the stability of the laminar flame, oscillations were introduced into the flame front by an external disturber. With a stable flame, the oscillations should have been damped--otherwise they might have been expected to spread. The experiments made were not sufficiently extensive to provide conclusive answers--nevertheless they will be described briefly.

Small cylinders used as external disturbers (shown in the duct in Figure 2 and in Figure 13) produced strong fluctuations in the unburned air stream (Ref. 5). A relatively small area of the flame directly in the wake of the cylinder was initially affected. In rich flames the disturbance spread rapidly laterally and within a short distance above the point of initial disturbance a large part of the flame surface was affected. With lean mixtures, the spread of the disturbance was much less (see Figures 28, 29 and 30) in some cases being reduced to a thin vertical band above the initial entry point of the turbulent wake.

For fixed fuel-air ratios the spread and strength of the turbulent flame area increased with Reynolds number of the disturbing cylinder (see Figures 13, 28 and 31). Spreading of the turbulence in

the flame was observed even at flow velocities as low as 10 ft/sec. When an 0.095 in. diameter rod was used to produce a turbulent wake, increased spread of the disturbance in the flame with increasing ϕ was even more evident (see Figures 32 and 33).

The resulting disturbance in the flame front consisted largely of waves between 0.1 in. and 0.3 in. in size. The experiments did not determine conclusively whether or not these waves had any relation to the 0.27 in. wave found in the undisturbed conical flame.

Although no firm correlation was possible between the two sets of waves--those generated by an external disturber and those present in the flame with no disturbance--these final experiments did yield interesting information on the flame stability. Here again the stability of the flame decreased with increasing speed of the upstream flow. The behavior of the flame with changing fuel-air was, however, puzzling. The observation that a lean flame was apparently less sensitive to external disturbances was not easily reconciled with the observation that the annular wave appeared less stable in lean flames than in rich. Aside from this one difficulty, a consistent picture of flame stability was obtained from all the experiments of this investigation. The flow velocities from 5 to 35 ft/sec covered in these experiments included the interesting transition range between laminar and completely turbulent flames. At these speeds the completely turbulent type of flame was not observed in the region close to the flame holder unless there were external disturbances. Further downstream, however, there were indications of true turbulent flames. In the intermediate speed range between 10 and 35 ft/sec

a moderately stable wave state of the flame front was found. Between these flow velocities the length of the wave was practically invariant for all conditions. This wave was apparently associated with the flame itself.

It was clear throughout the investigations that the stability of the flame decreased with increasing flow velocity. The flame front was laminar at low velocities; then at a slightly higher velocity it became unstable and entered another stable state. Finally, at high speeds it is known that the flame front is completely turbulent.

REFERENCES

1. Landau, L., Acta Physicochim., U.R.S.S., 19, 77, (1944).
2. Markstein, G. H., J. Aero. Sci., 18, 199, (1951).
3. Karlovitz, B., Denniston, D. W. Jr., and Wells, F. E., "Investigation of Turbulent Flames", J. Chem. Phys., 19, 541, (1951).
4. Roshko, A., "On the Development of Turbulent Wakes from Vortex Streets", Thesis, Calif. Inst. of Tech., (1952).
5. Möller, "Photographic and Kinematographic Investigations of a Wake Behind a Sphere", Physik. Zeitschr., 39, 57-66, (1938).

NOMENCLATURE

- d = diameter of spherical flame holder (in)
- h = amplitude of annular wave in flame front (in)
- l = distance from flame holder measured along flame front (in)
- l_o = distance of first noticeable wave in flame front from flame holder (in)
- n = frequency of annular wave in flame front (sec^{-1})
- r = radius of any point in 2.969 in. circular orifice (in)
- R = inside radius of circular orifice = 1.484 in.
- Re = Reynolds number = $\frac{\rho U_o d}{\mu} = \frac{U_o d}{\nu}$
- S_a = propagation velocity parallel to flame front
= vector sum of S_u and U_o (ft/sec)
- S_u = laminar flame propagation velocity (perpendicular to the flame front) (ft/sec)
- u = fluctuation velocity (ft/sec)
- U = velocity of the air at any point (ft/sec)
- \bar{U} = mean velocity of the air = $\frac{\text{volume flow rate}}{\text{area of cross section}}$ (ft/sec)
- U_{axial} = velocity of air at center of duct or orifice (ft/sec)
- U_o = mean velocity of the unburned air-propane gas mixture
= $\bar{U} (1 + \phi/23.8)$ (ft/sec)
- λ = wavelength of annular wave in flame front (in)
- $\bar{\lambda}$ = mean wavelength (in)
- μ = coefficient of viscosity
- ν = kinematic viscosity coefficient = μ/ρ
- ϕ = mixture equivalence ratio = fraction of stoichiometric propane-air mixture
= 23.8 x propane/air volume ratio
- ρ = density of a gas
- θ = angle that the conical flame front makes with the vertical where there are no flame holder support wire effects
- θ' = angle of conical flame front where it is in the wake of the support wire

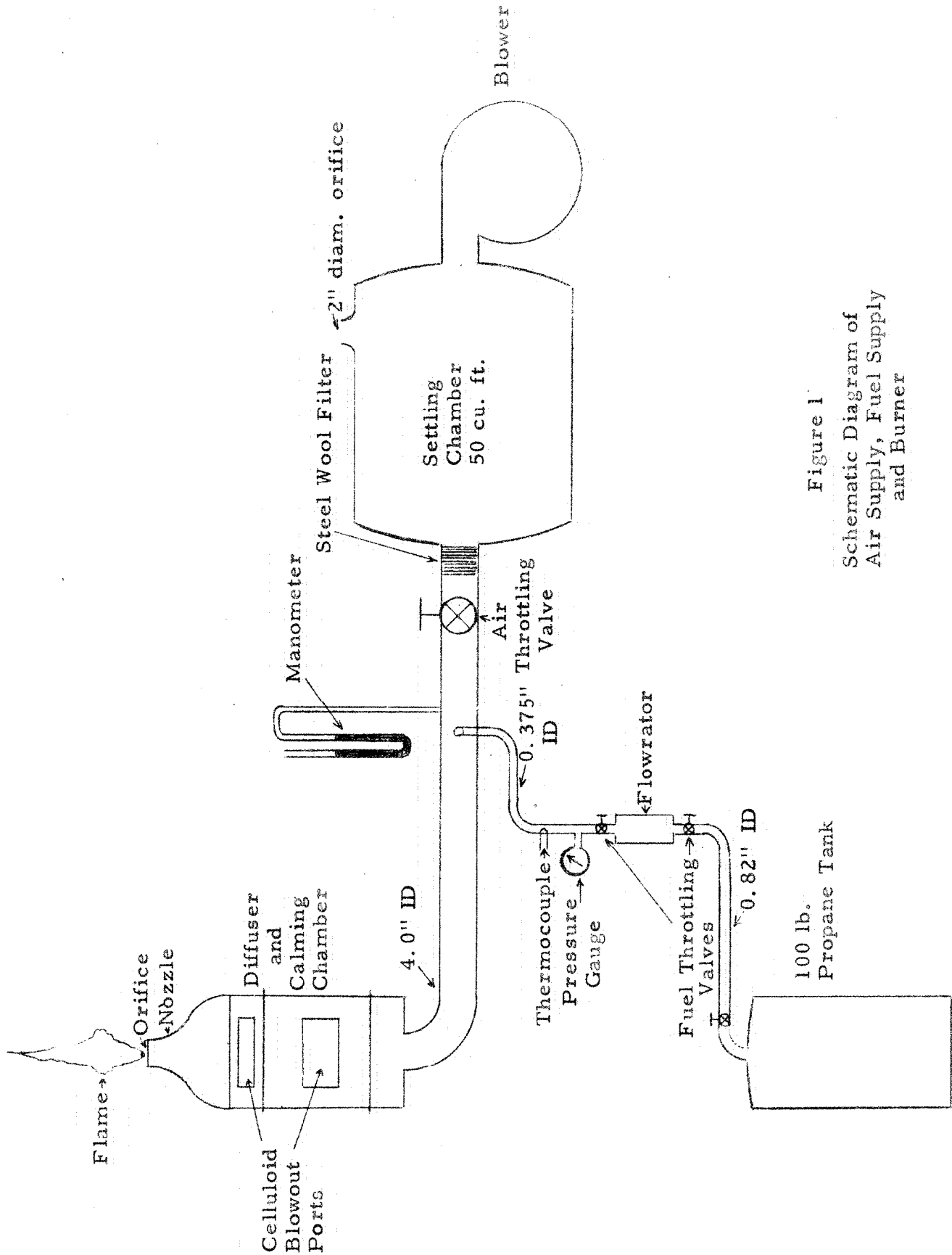


Figure 1
Schematic Diagram of
Air Supply, Fuel Supply
and Burner

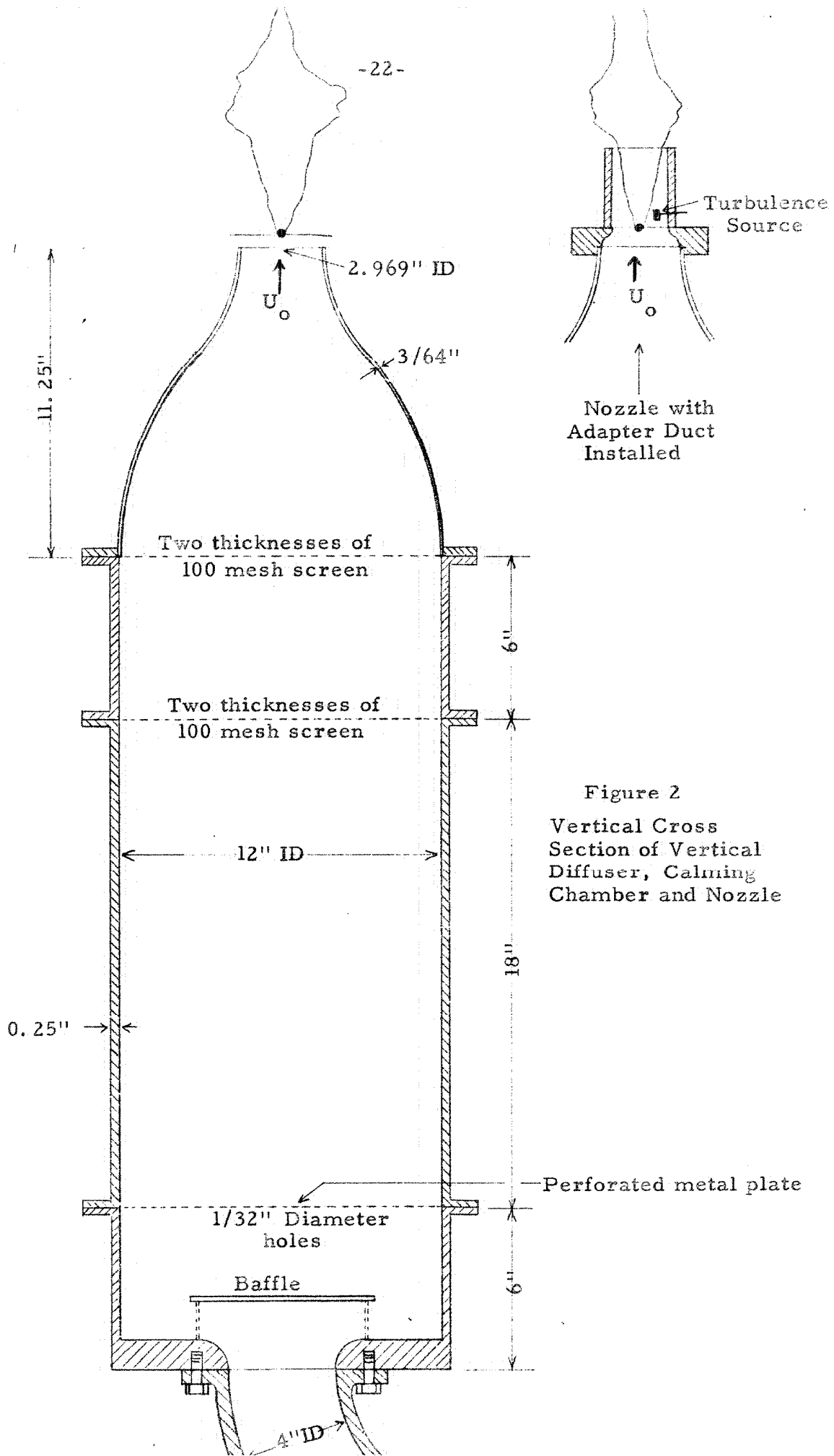


Figure 2
 Vertical Cross
 Section of Vertical
 Diffuser, Calming
 Chamber and Nozzle

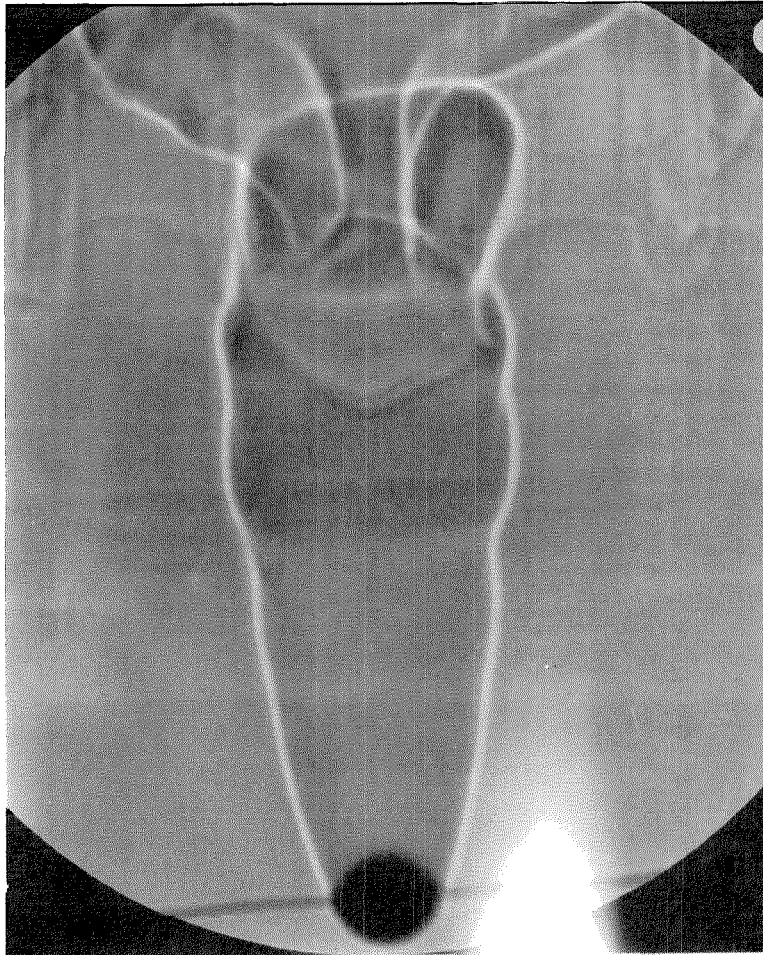
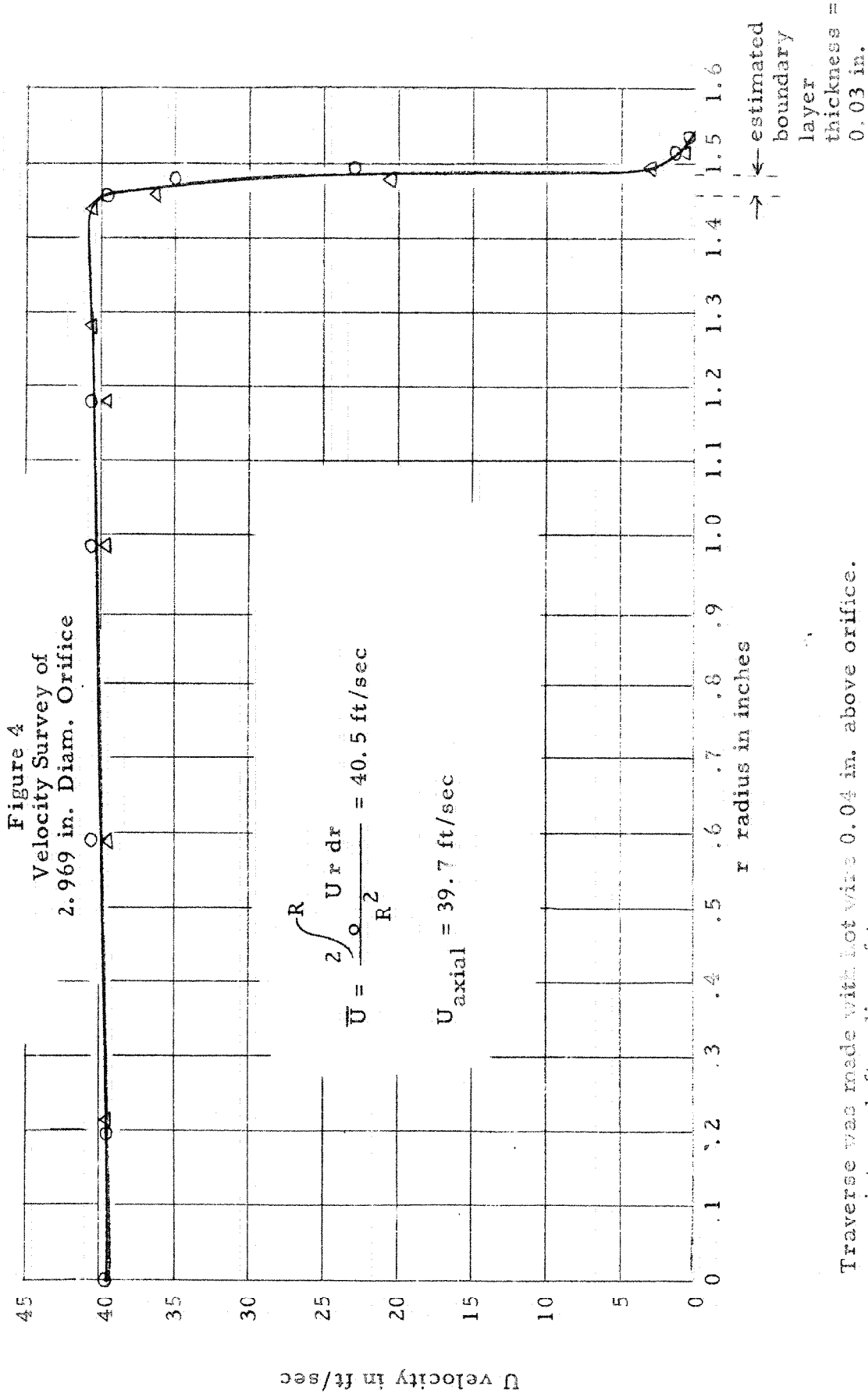


Figure 3
Example of a Lean Conical Flame
Showing the Flame Holder and Support Wire
Flame Front Wave Well Developed
 $U_o = 18.4$ ft/sec
 $\phi = 0.63$
0.25 in. Diameter Flame Holder



Traverse was made with hot wire 0.04 in. above orifice.
 o - points on left radius of traverse
 Δ - points on right radius of traverse

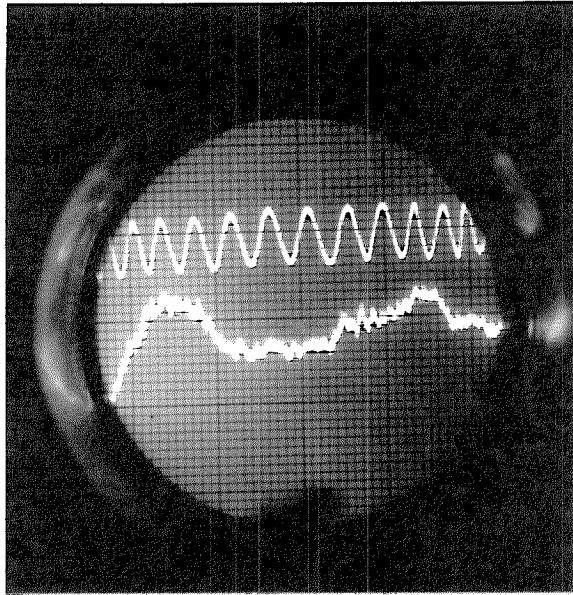


Figure 5
Upstream Flow Velocity Fluctuations
(Signal Obtained from a Hot Wire Anemometer)
 $U_o = 30.0$ ft/sec
Calibrating Signal = 1200 cycles/sec

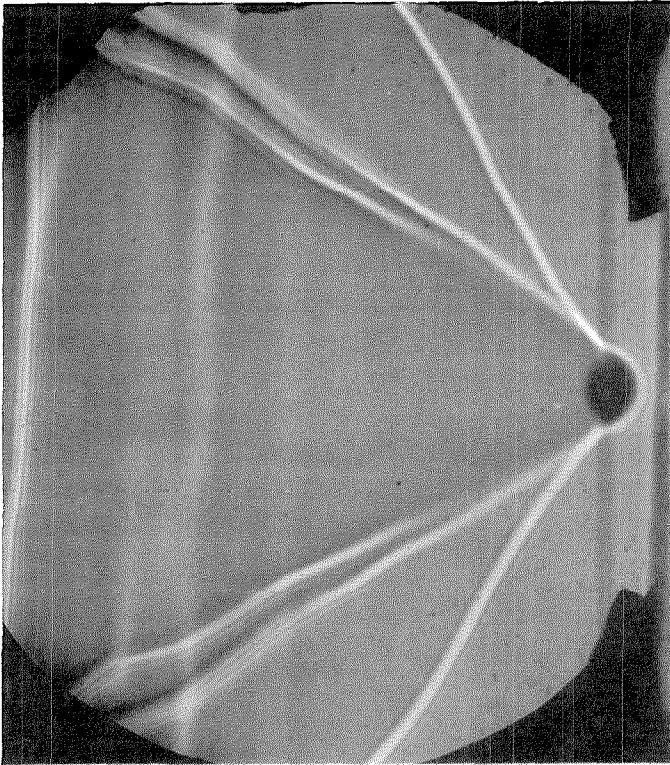


Figure 6

Front View of Typical Flame

Showing Support Wire Wake Effect

$$U_o = 6.7 \text{ ft/sec}$$

$$\phi = 1.05$$

0.125 in. Diameter Flame Holder

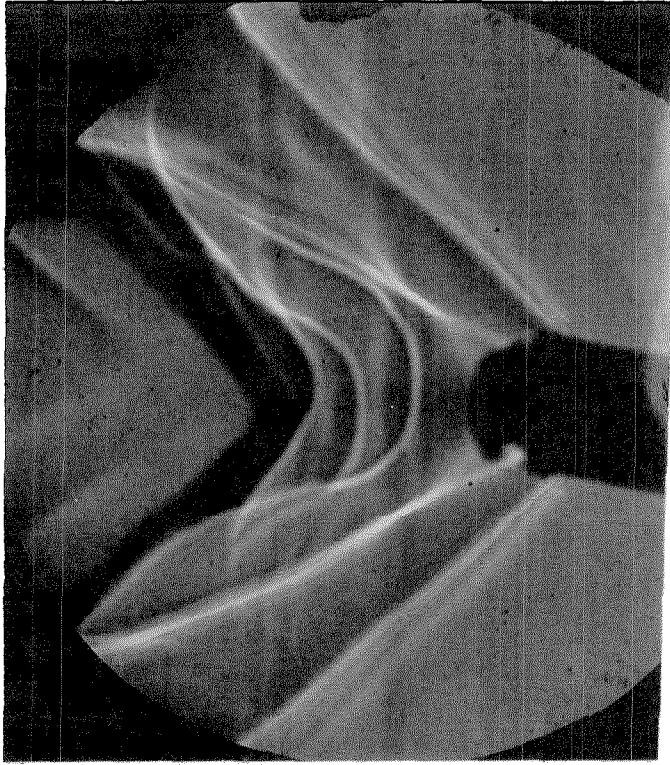


Figure 7

Side View of Typical Flame

Showing Support Wire Wake Effect

$$U_o = 6.7 \text{ ft/sec}$$

$$\phi = 1.05$$

0.125 in. Diameter Flame Holder

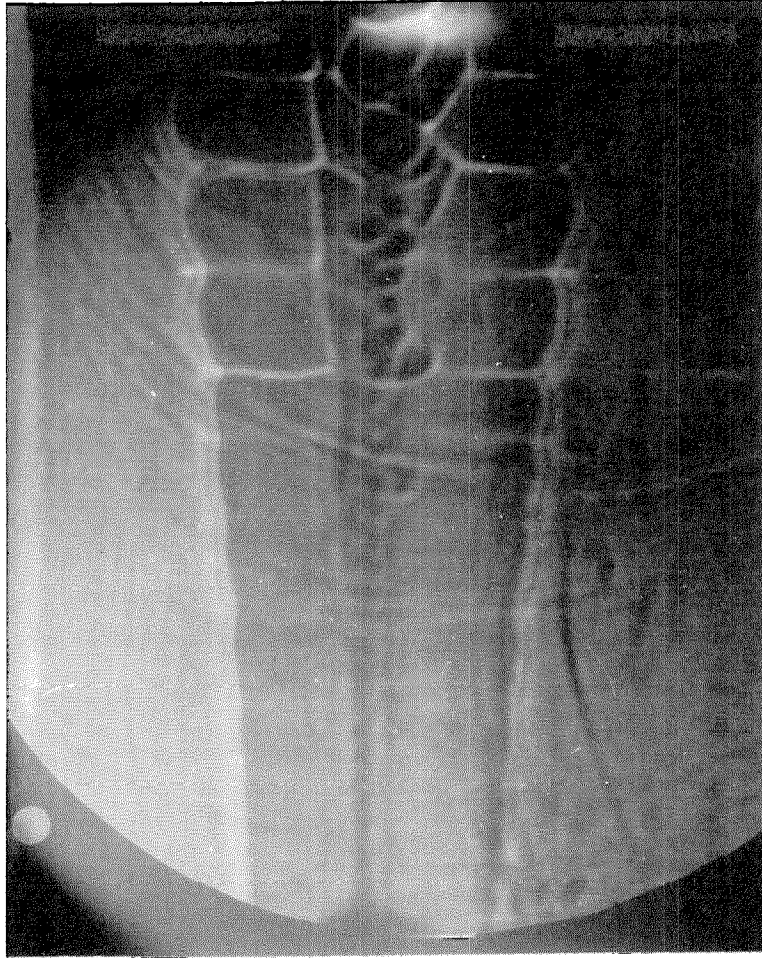


Figure 8
Vortex Street in Flame
in the Wake of the Support Wire
 Re of Support Wire = 162
 $U_o = 29.7$ ft/sec
 $\phi = 1.09$
0.5 in. Diameter Flame Holder

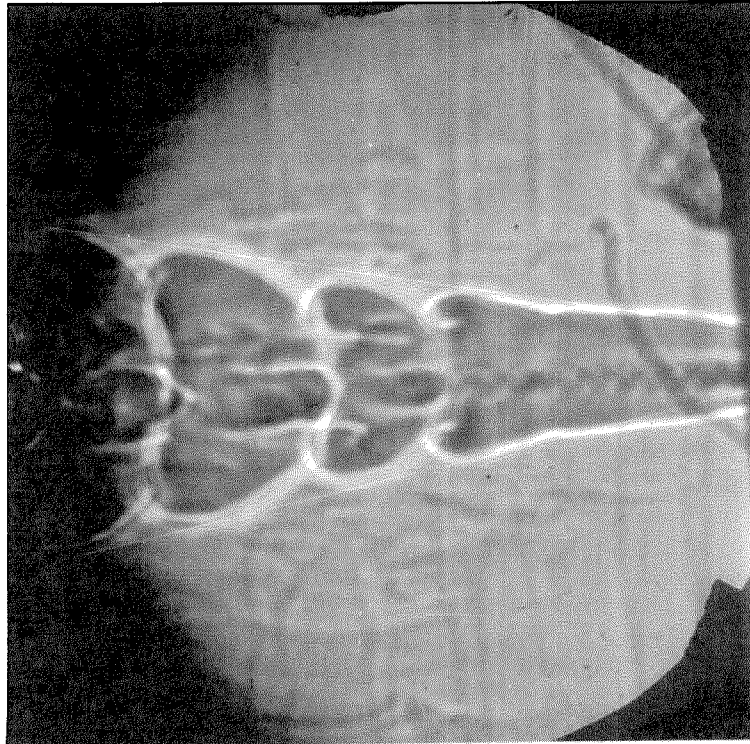


Figure 9

Vortex Street in Flame and
Well Developed Annular Flame Front Wave

Re of Support Wire = 70

$U_o = 26.6$ ft/sec

$\phi = 0.75$

0.125 in. Diameter Flame Holder

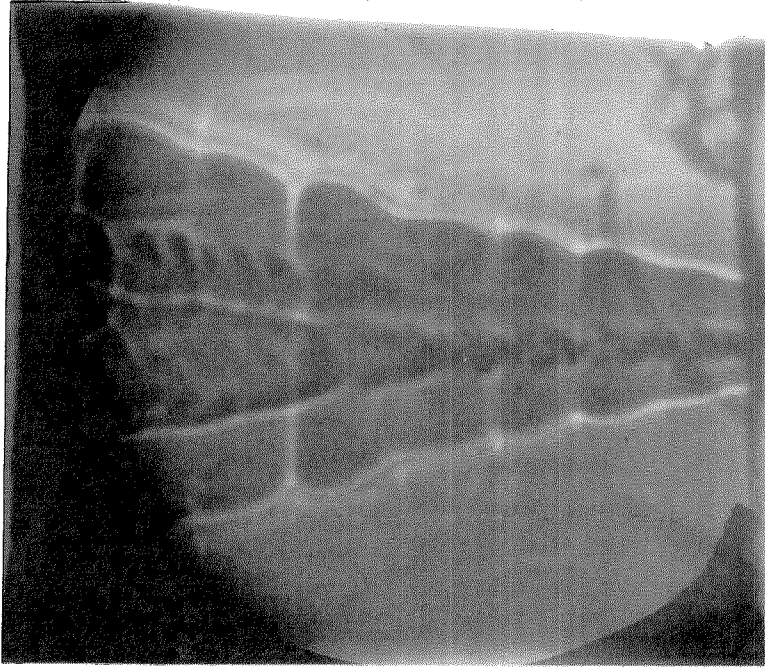


Figure 10

Vortex Streets on Near and Far Face
of Flame Visible
(Support Wire Was Not Quite Parallel
to the Line of Sight)

Re of Support Wire = 61

$U_o = 24.1$ ft/sec

$\phi = 1.00$

1.125 in. Diameter Flame Holder

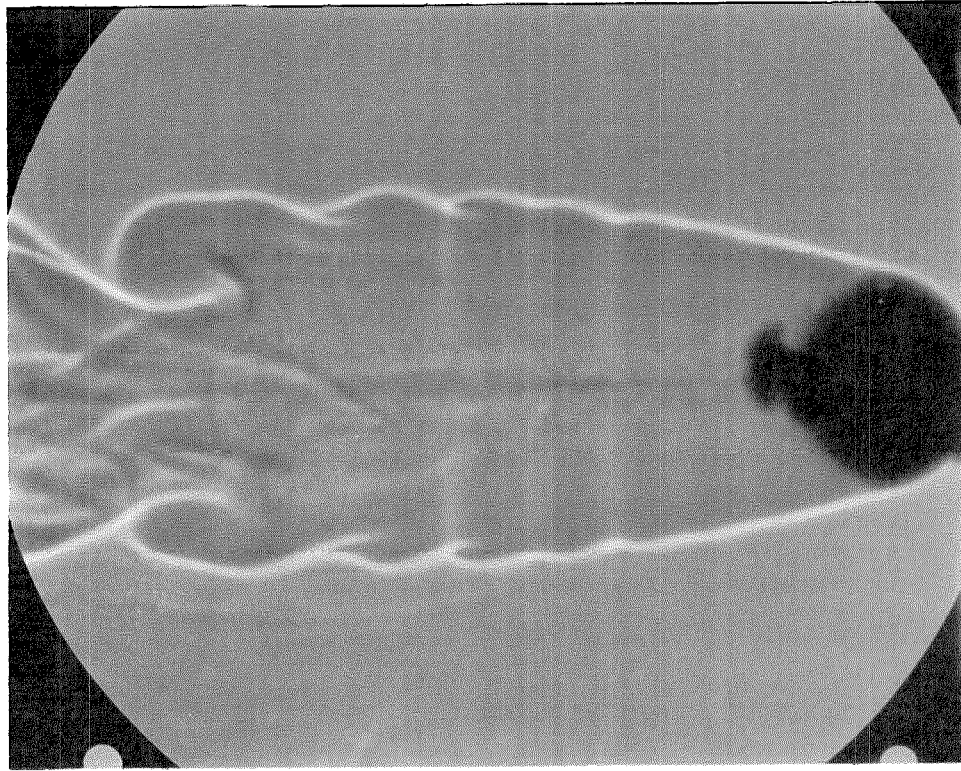


Figure 11

Vortex Street in Flame and
Rolled Up Flame Front Wave
Typical of Very Lean Flames
Re of Support Wire = 90

$U_0 = 18.3$ ft/sec
 $\phi = 0.57$

0.5 in. Diameter Flame Holder

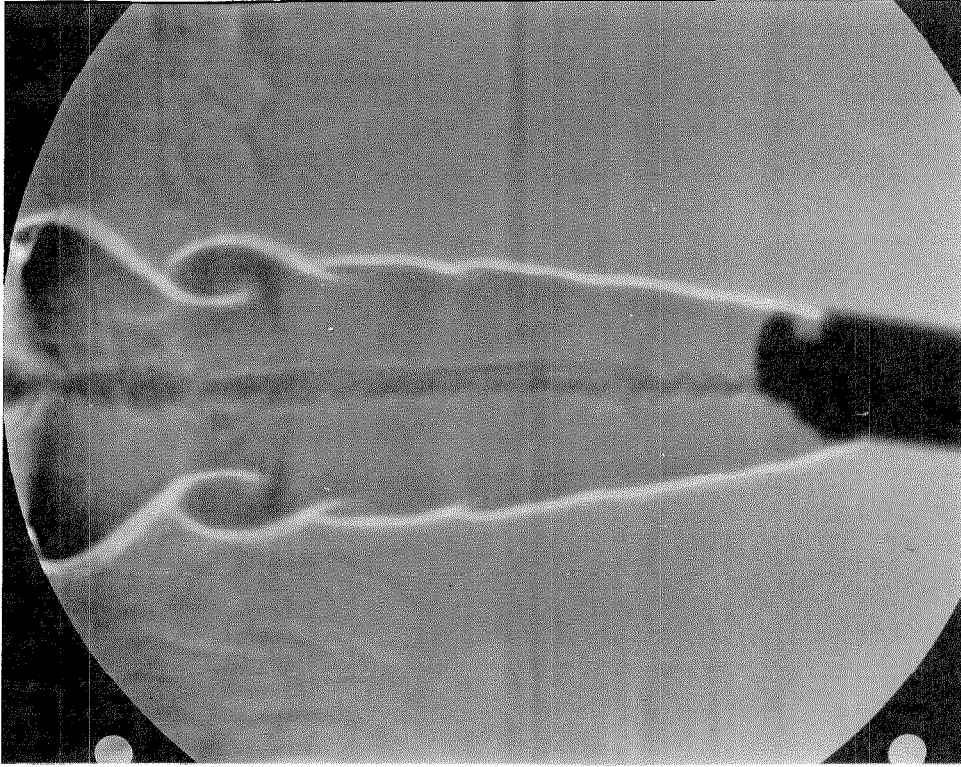


Figure 12

Vortex Street in Flame
and Rolled Up Flame Front Wave
Re of Support Wire = 45

$U_0 = 18.4$ ft/sec
 $\phi = 0.63$

0.25 in. Diameter Flame Holder

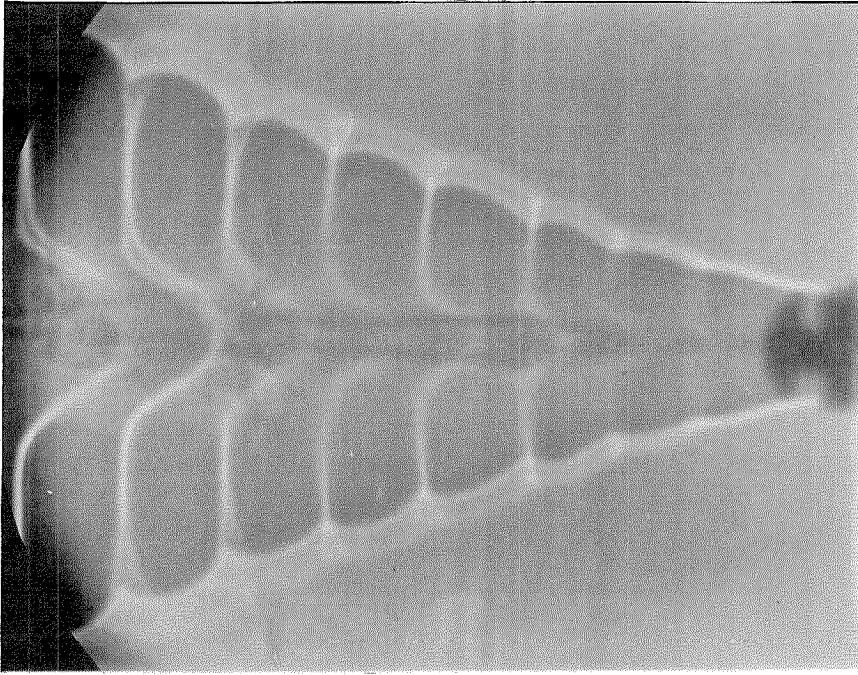


Figure 14
Typical Example of the Regular
Annular Flame Front Wave
 $U_o = 17.5$ ft/sec
 $\phi = 0.83$
0.125 in. Diameter Flame Holder

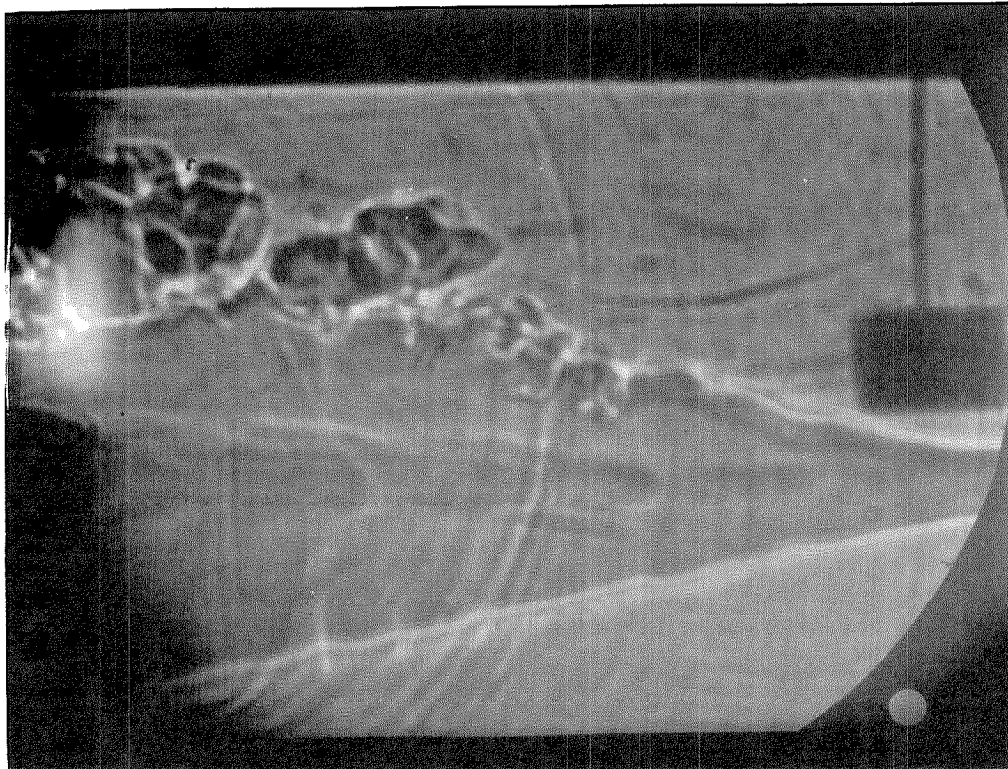
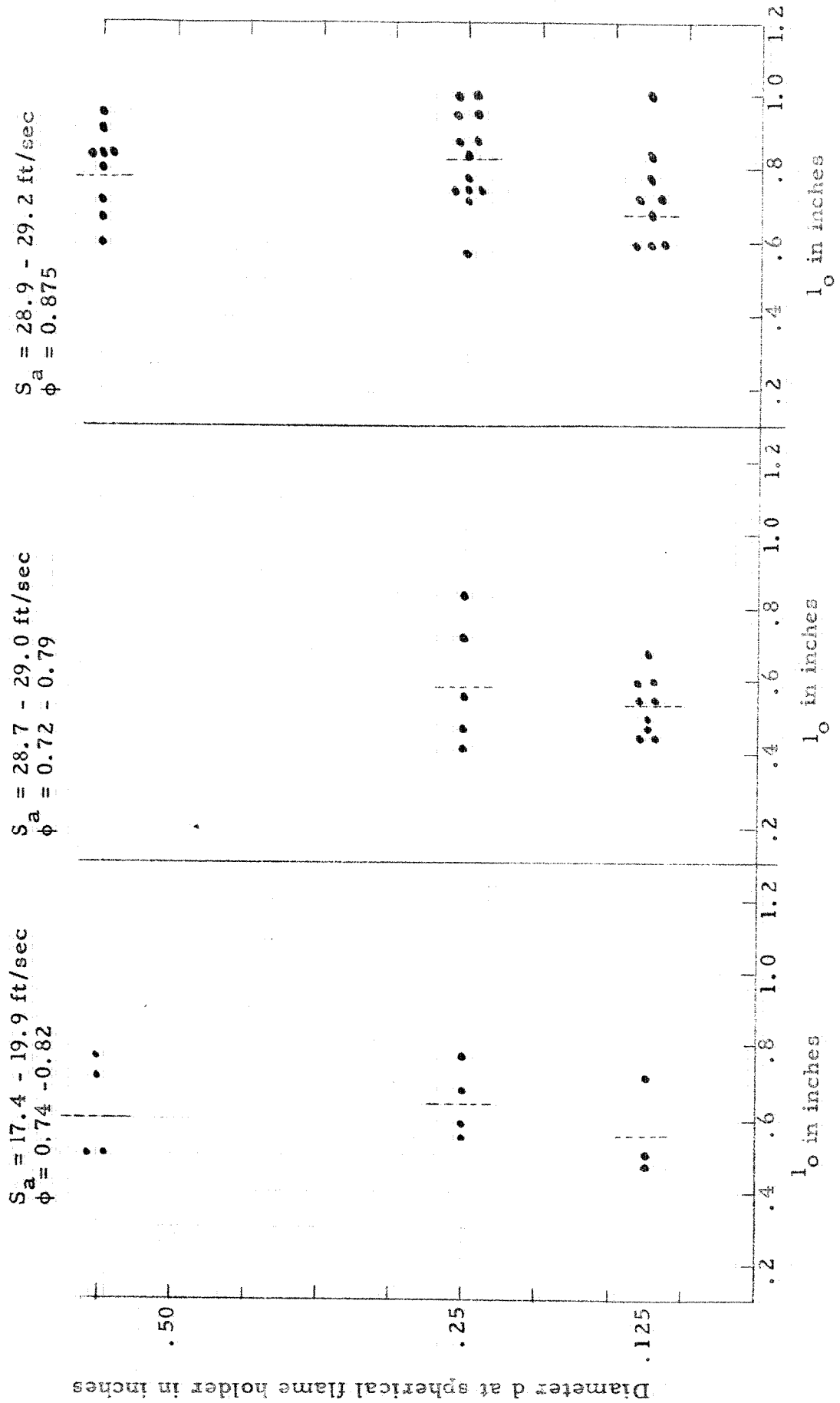


Figure 13
Flame Front Disturbed by a
Turbulent Wake of a Bluff Body
0.25 in. Diameter Turbulence Source
 $U_c = 29.4$ ft/sec
 $\phi = 0.87$

Figure 15

Typical Examples Showing that the Distance l_0
is Essentially Independent of Flame Holder Size



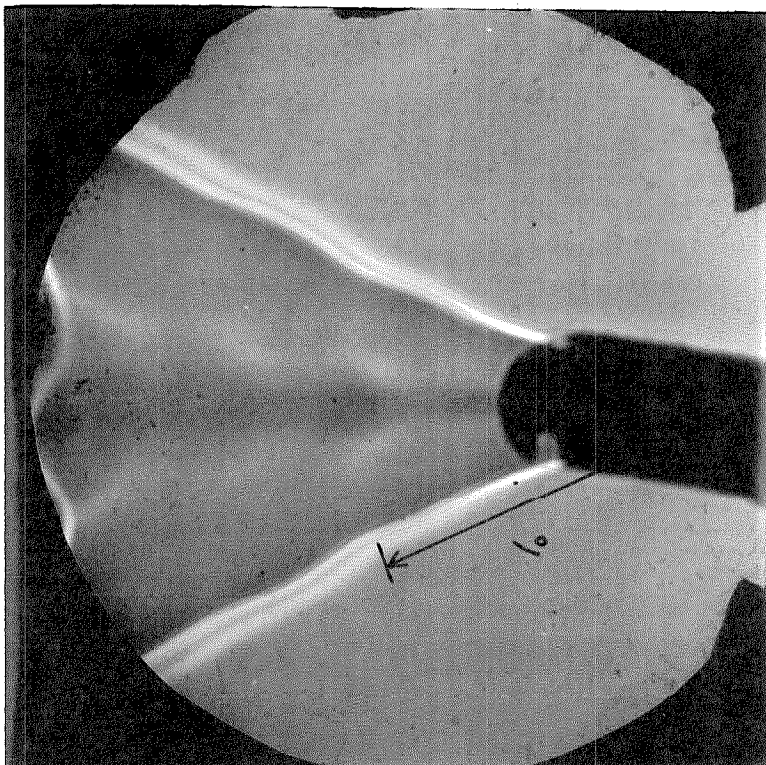


Figure 16
Annular Flame Front Waves
(Note distance l_0 where they
are first noticeable)

$l_0 = 0.75$ in.
 $U_0 = 6.6$ ft/sec
 $\phi = 0.87$
0.125 in. Diameter Flame Holder

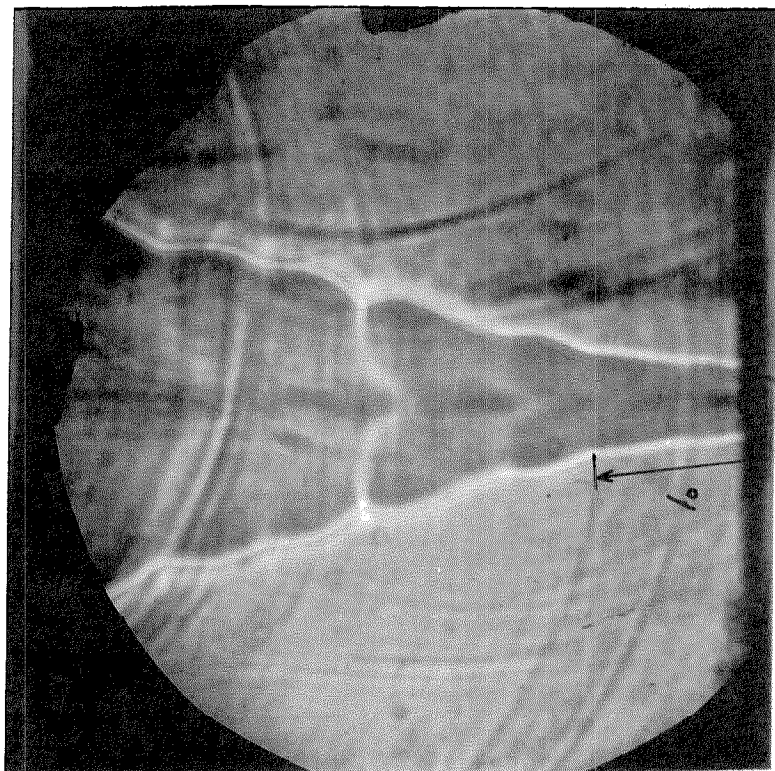


Figure 17
Annular Flame Front Waves
(Note distance l_0)

$l_0 = 0.45$ in.
 $U_0 = 14.2$ ft/sec
 $\phi = 0.86$
0.125 in. Diameter Flame Holder

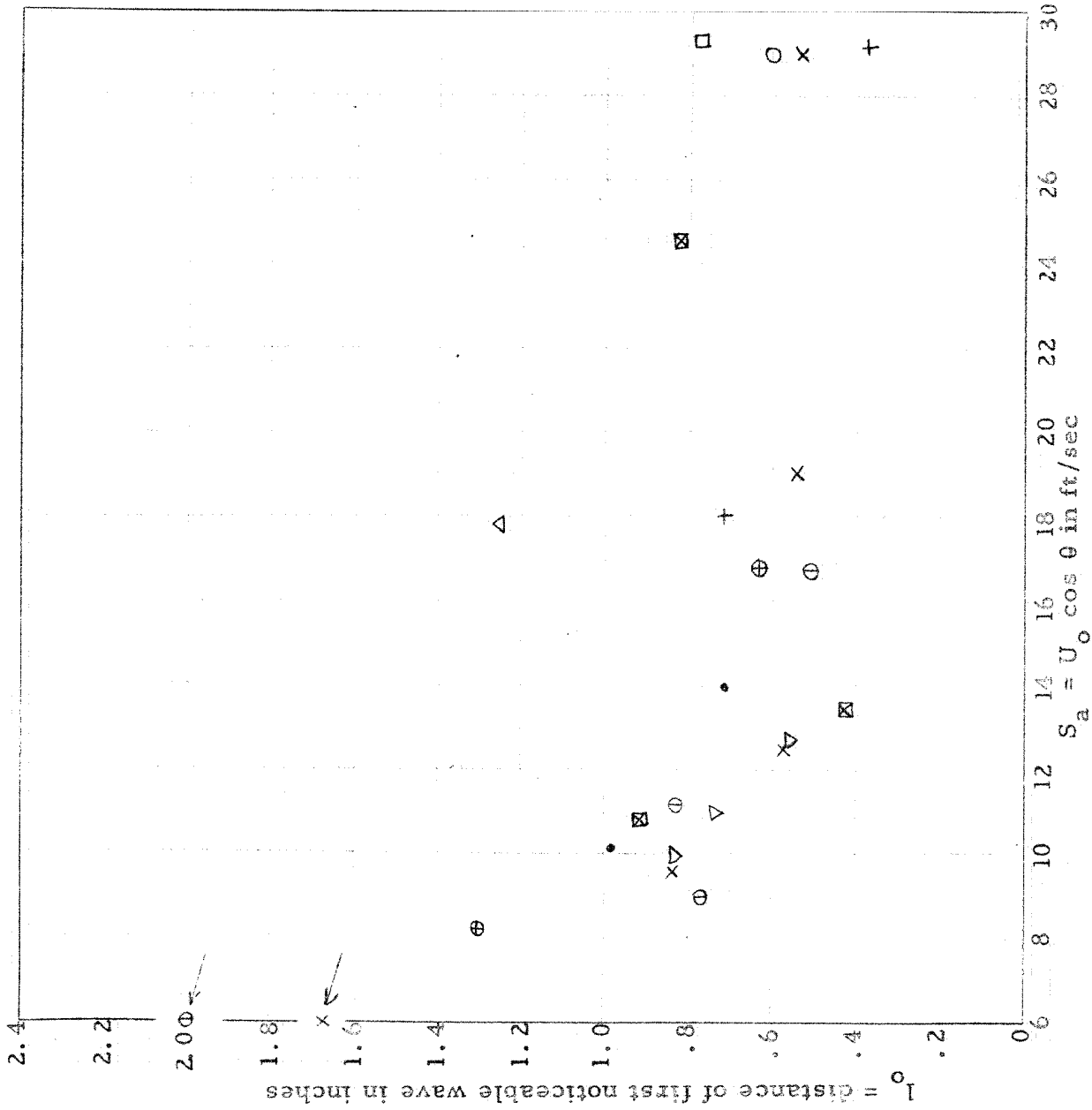


Figure 18
 Plot Showing Decrease in
 Distance l_0 of First Notice-
 able Wave with Increase in
 Propagation Velocity Par-
 allel to the Flame Front S_a

ϕ = Mixture Equivalence
 Ratio

- + $\phi = 0.57 - 0.69$
- x $= 0.70 - 0.79$
- ⊙ $= 0.80 - 0.89$
- ⊕ $= 0.90 - 0.99$
- $= 1.00 - 1.09$
- ⊗ $= 1.10 - 1.19$
- △ $= 1.20 - 1.29$
- ▽ $= 1.30 - 1.39$
- $= 1.40 - 1.53$

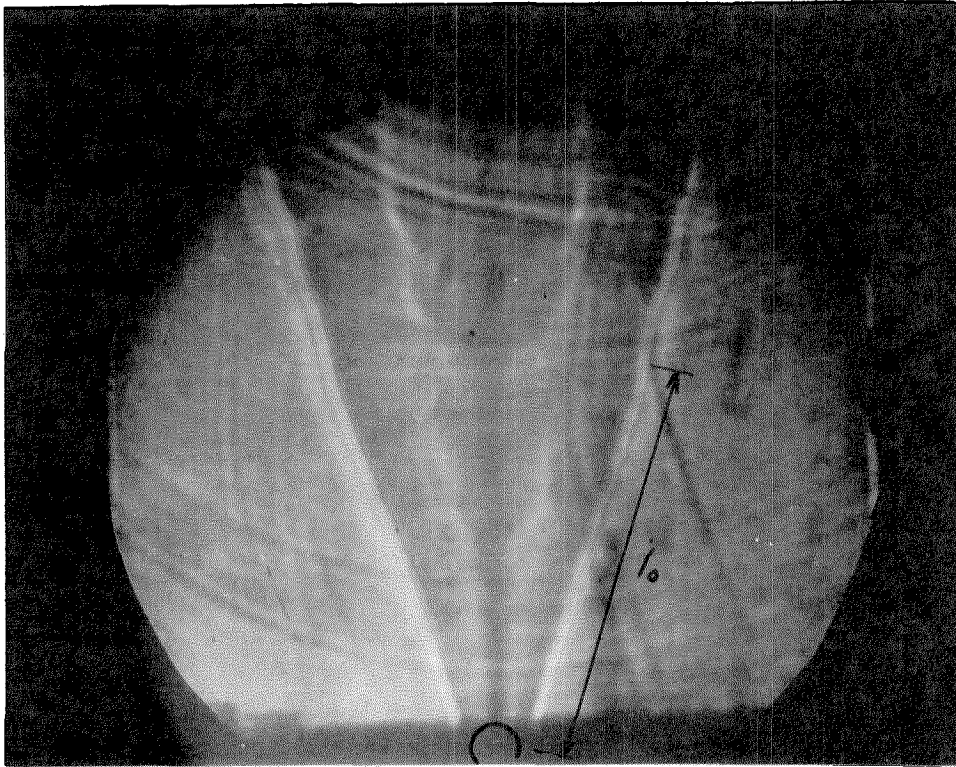
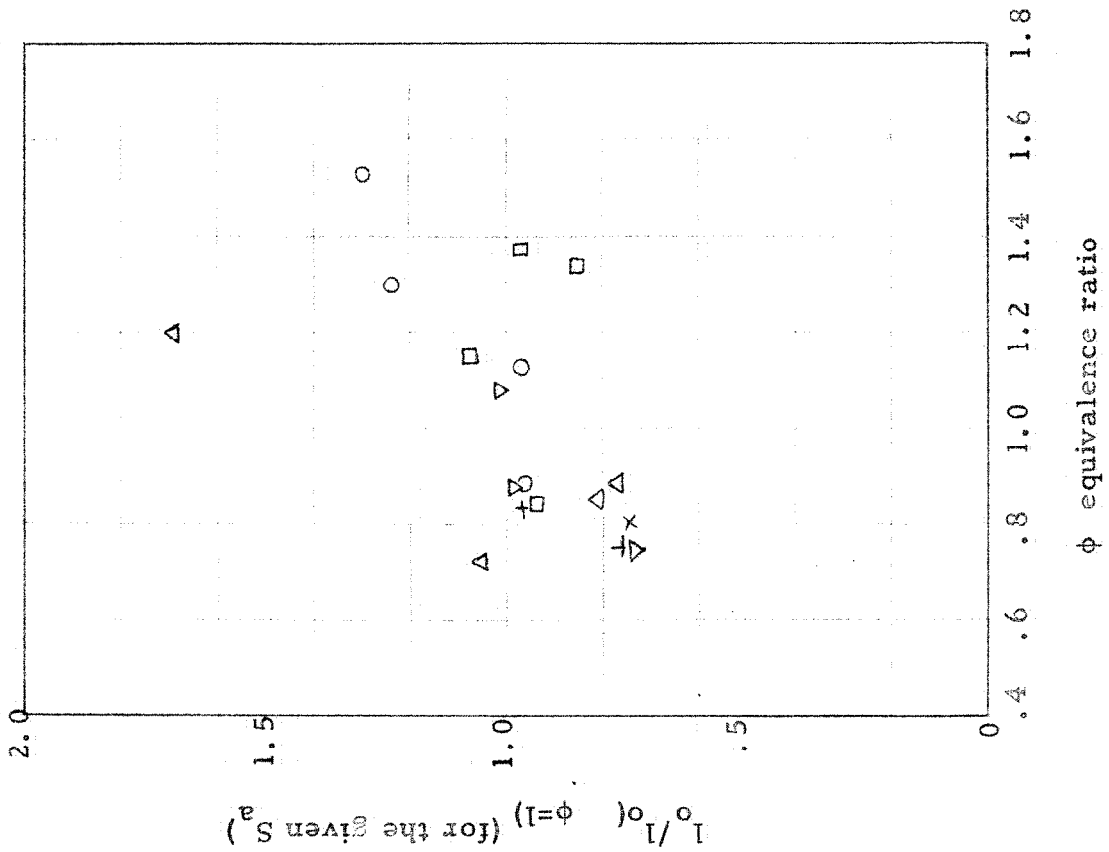


Figure 19
Annular Flame Front Waves
(Note distance l_0 where they
are first noticeable)
 $l_0 = 1.0$ in.
 $U_0 = 14.4$ in.
 $\phi = 1.30$
0.125 in. Diameter Flame Holder

Figure 20
 Plot Showing Increase in Distance l_0
 of First Noticeable Wave with In-
 crease in Mixture Equivalence Ratio ϕ

$S_a = U_o \cos \theta$ in ft/sec
 x $S_a = 5.0 - 6.0$
 + $= 8.0 - 9.0$
 □ $= 10.0 - 12.0$
 ○ $= 13.0 - 15.0$
 Δ $= 16.0 - 18.0$
 ▽ $= 28.0 - 29.4$



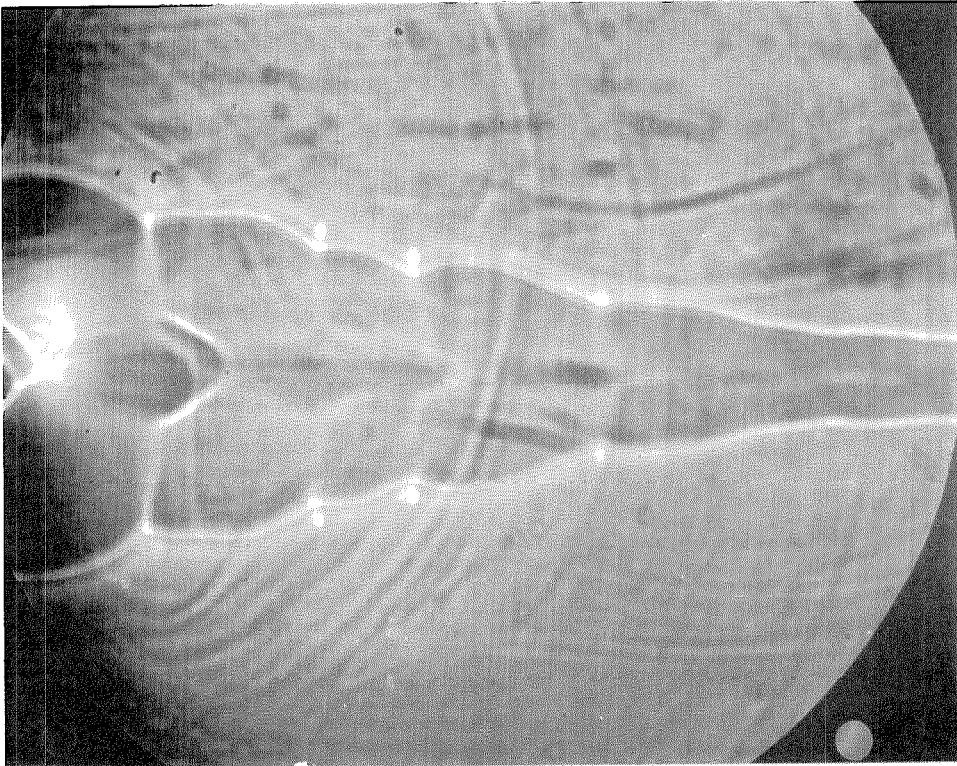


Figure 21
Amplitude Development of Flame
Front Waves
 $U_0 = 29.3 \text{ ft/sec}$
 $\phi = 0.79$
0.125 in. Diameter Flame Holder

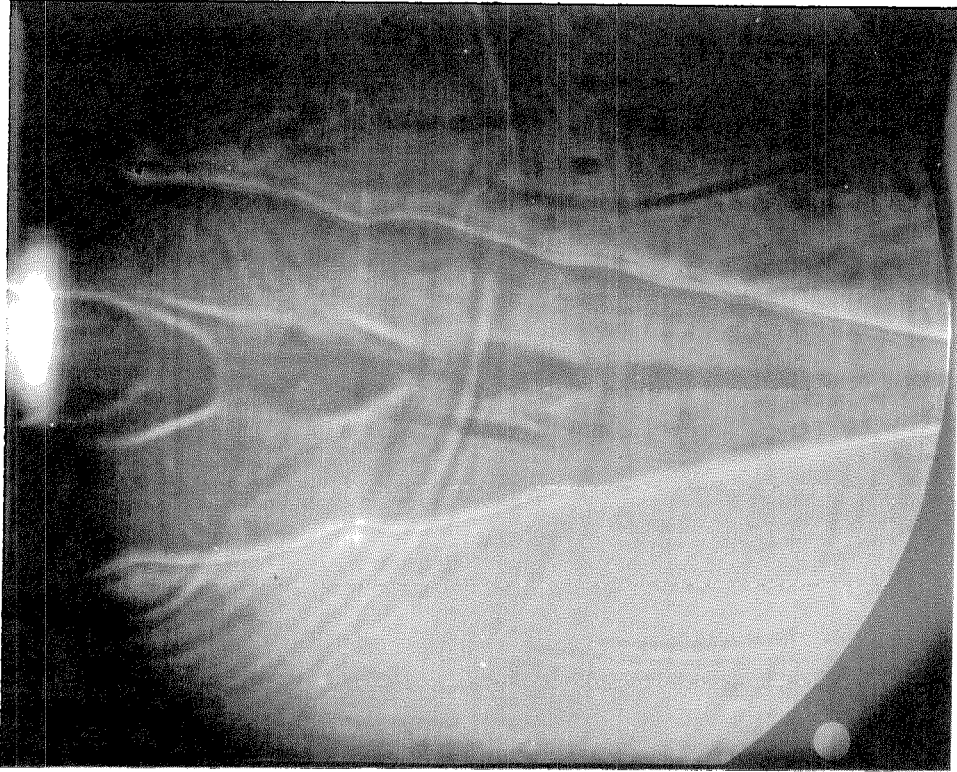


Figure 22
Amplitude Development of
Flame Front Waves
 $U_0 = 29.4 \text{ ft/sec}$
 $\phi = 0.87$
0.125 in. Diameter Flame Holder

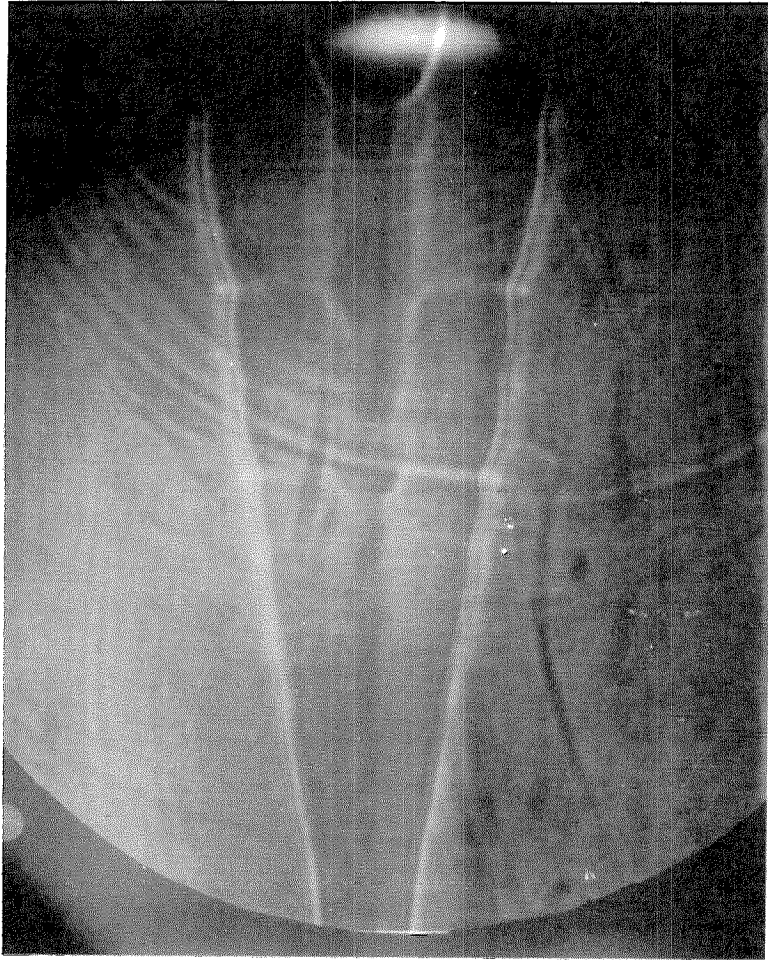


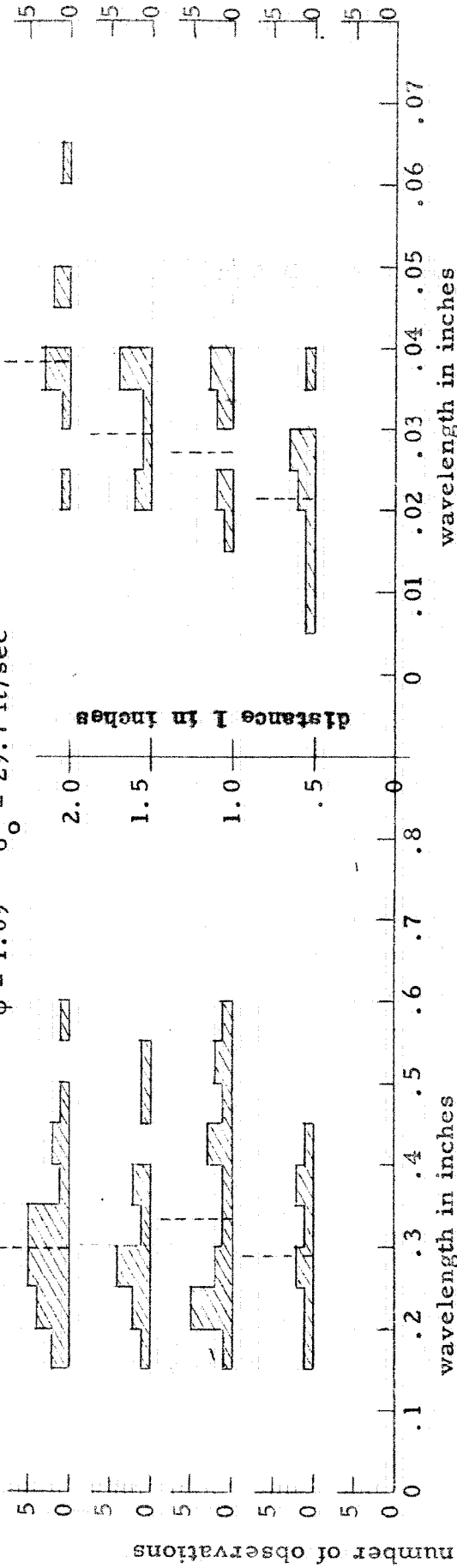
Figure 23
Amplitude Development of
Flame Front Waves
 $U_o = 29.7 \text{ ft/sec}$
 $\phi = 1.09$
0.125 in. Flame Holder

Figure 24

Histogram of Wavelength versus Distance from Flame Holder

Histograms of Wave Amplitude versus Distance l from Flame Holder

0.125 in. Spherical Flame Holder
 $\phi = 1.09$ $U_0 = 29.7$ ft/sec



0.125 in Spherical Flame Holder
 $\phi = 0.79$ $U_0 = 29.3$ ft/sec

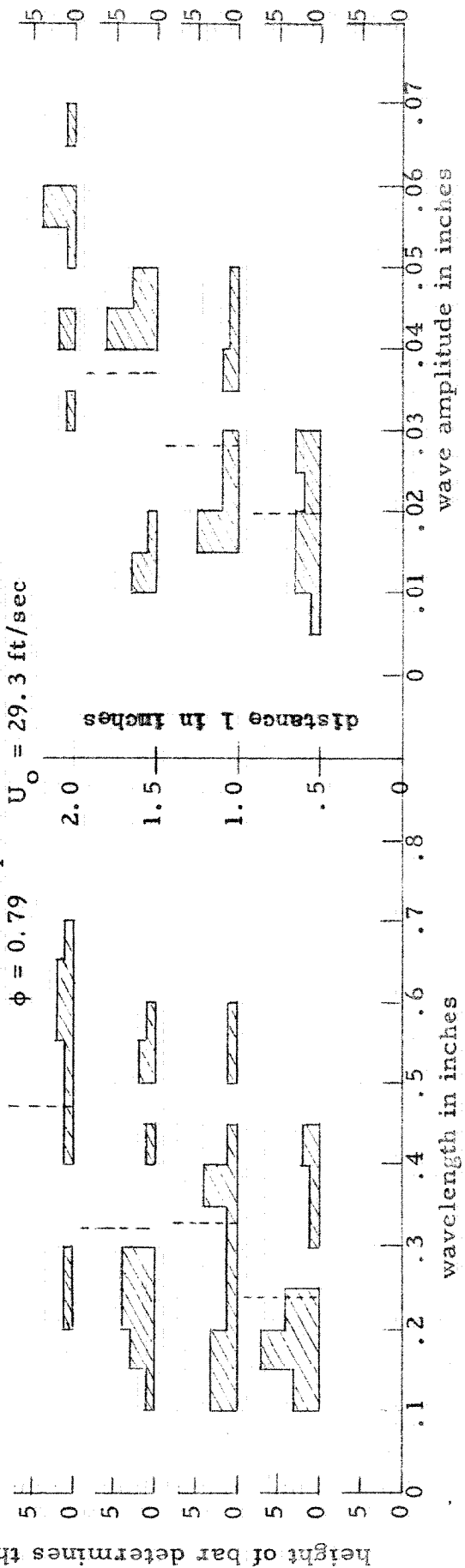
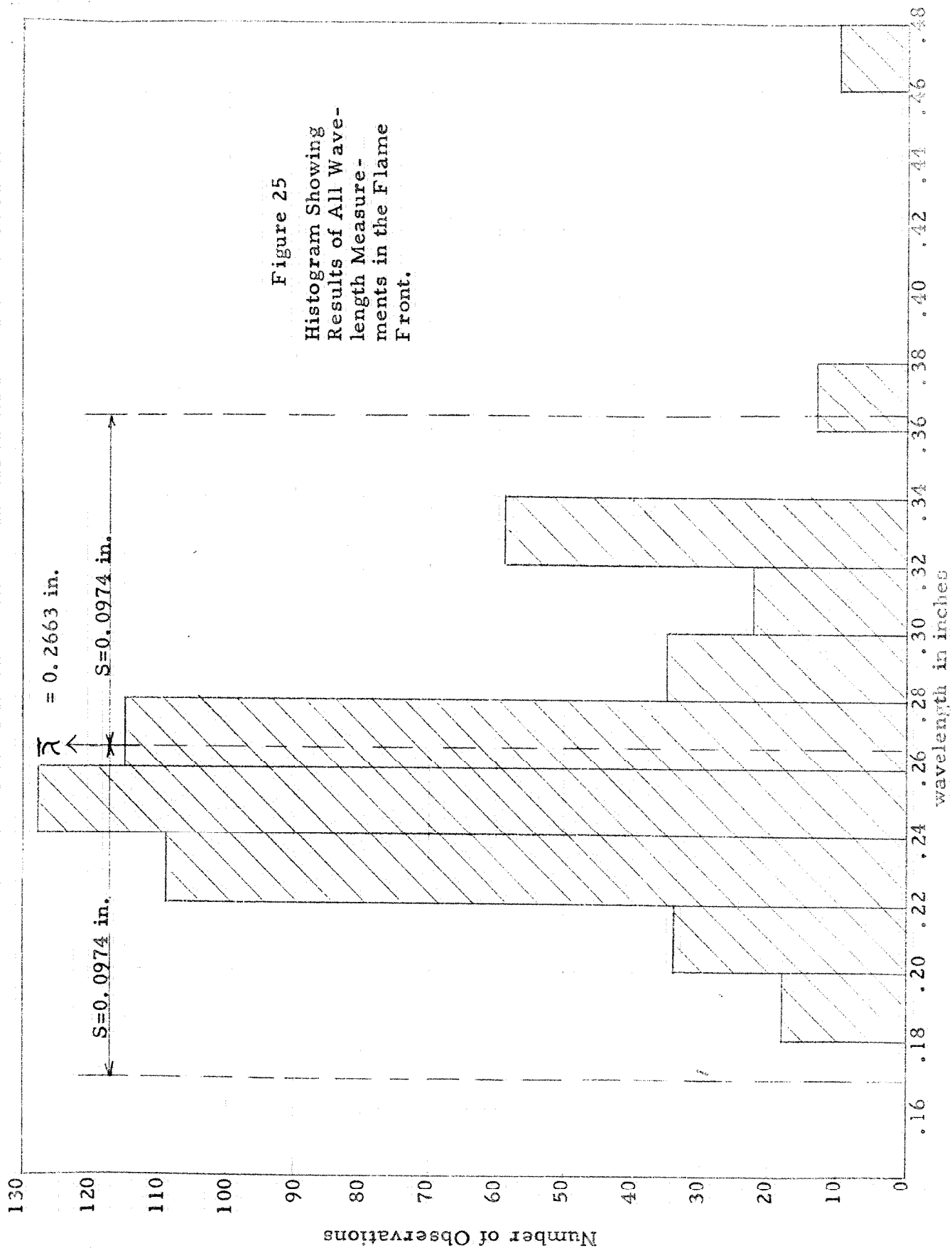


Figure 25
Histogram Showing
Results of All Wave-
length Measure-
ments in the Flame
Front.



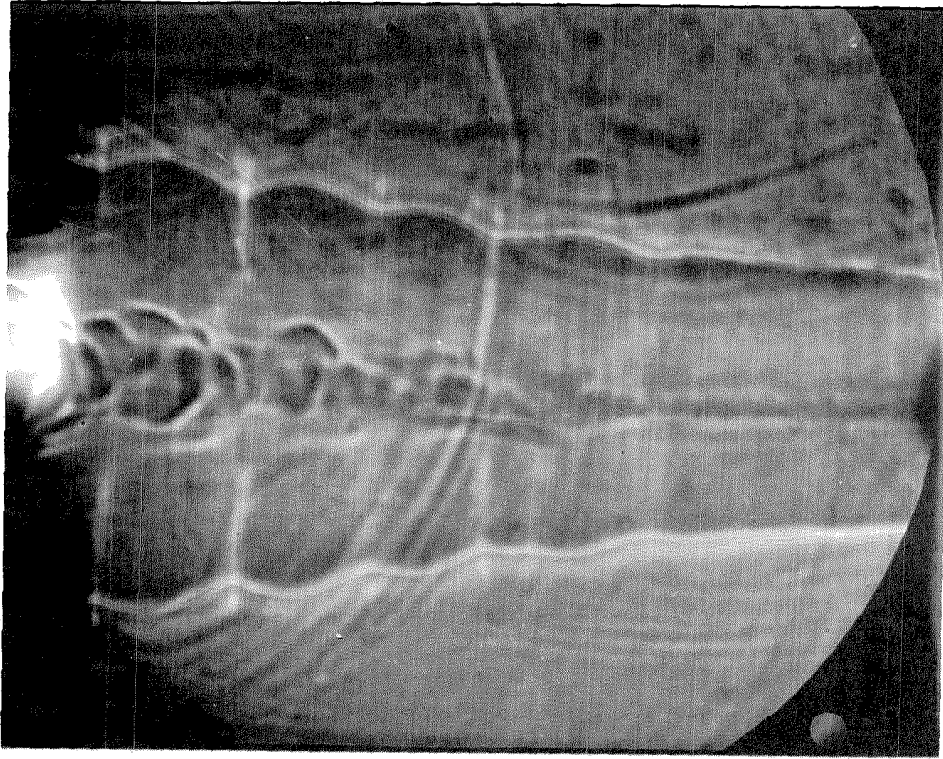


Figure 27

Constant Flame Front Wavelength

$$U_0 = 30.3 \text{ ft/sec}$$

$$\phi = 0.87$$

0.5 in. Diameter Flame Holder

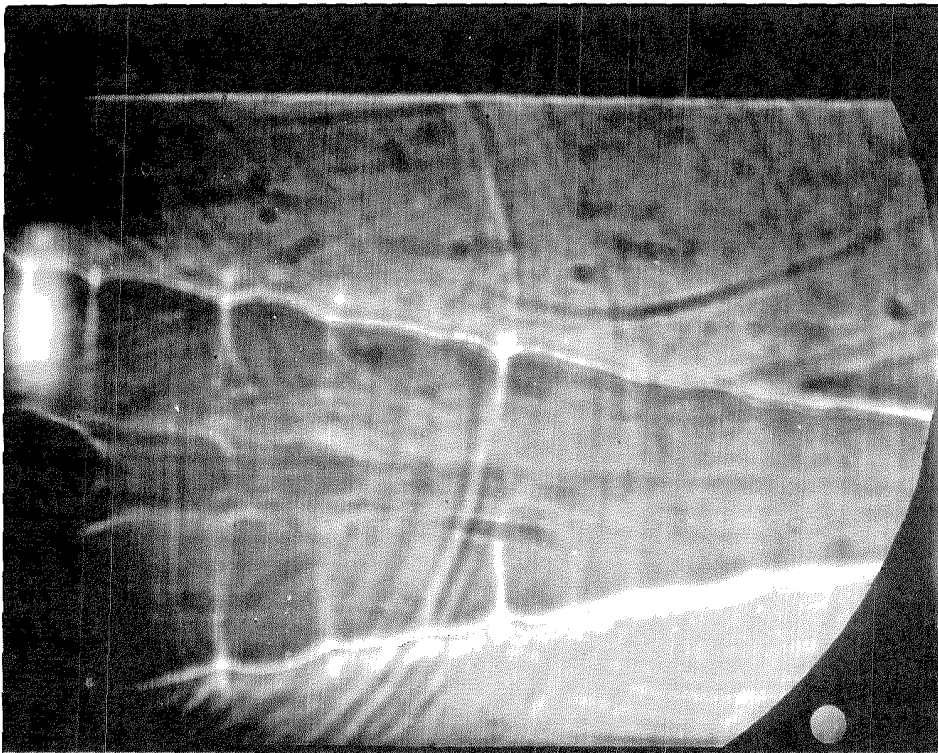


Figure 26

Constant Flame Front Wavelength

$$U_0 = 29.4 \text{ ft/sec}$$

$$\phi = 0.87$$

0.25 in. Diameter Flame Holder

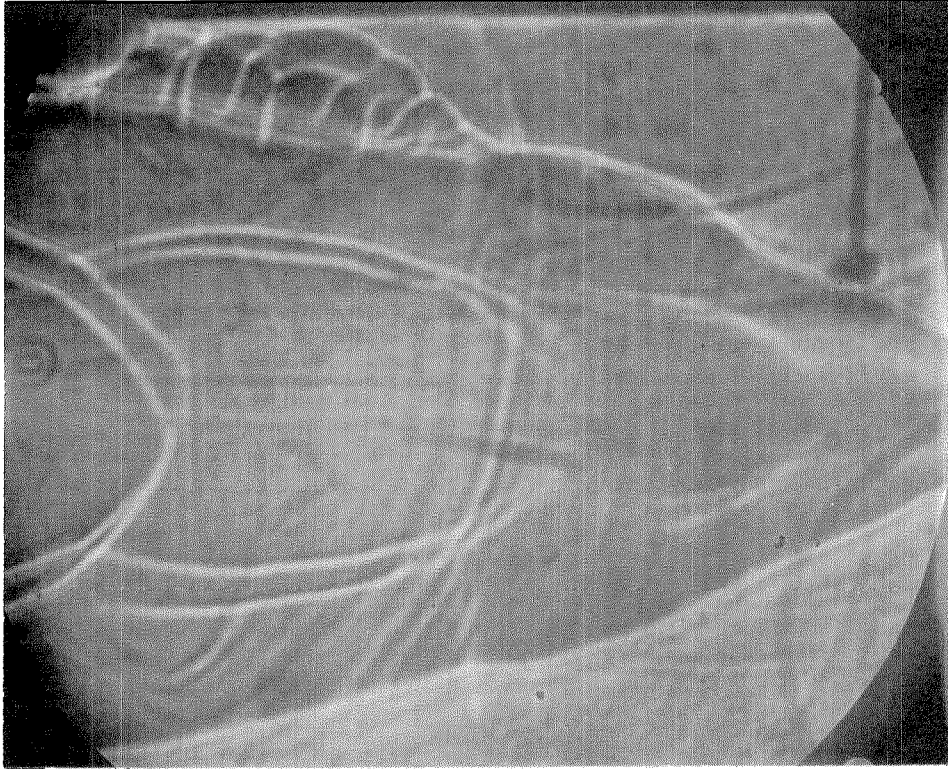


Figure 29

Effect of Turbulent Wake on Flame Front

0.065 in. Diameter Turbulence Source

$U_o = 11.6$ ft/sec

$\phi = 1.16$

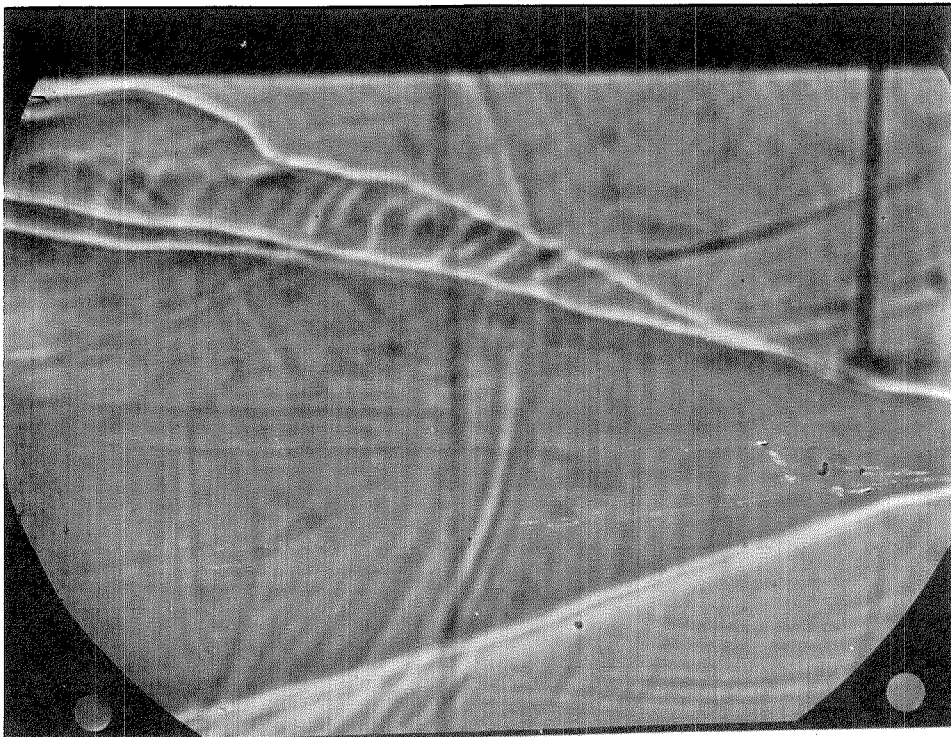


Figure 28

Effect of Turbulent Wake on Flame Front

0.065 in. Diameter Turbulence Source

$U_o = 11.6$ ft/sec

$\phi = 0.84$

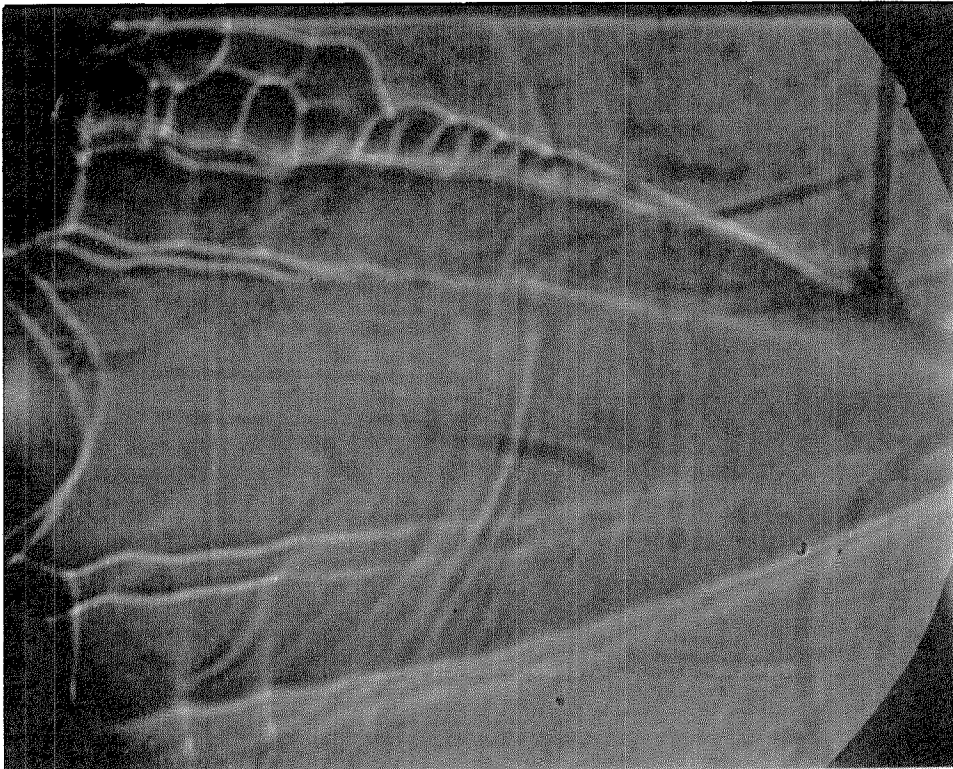


Figure 30

Effect of Turbulent Wake on Flame Front

0.065 in. Diameter Turbulence Source

$U_o = 11.8$ ft/sec

$\phi = 1.33$

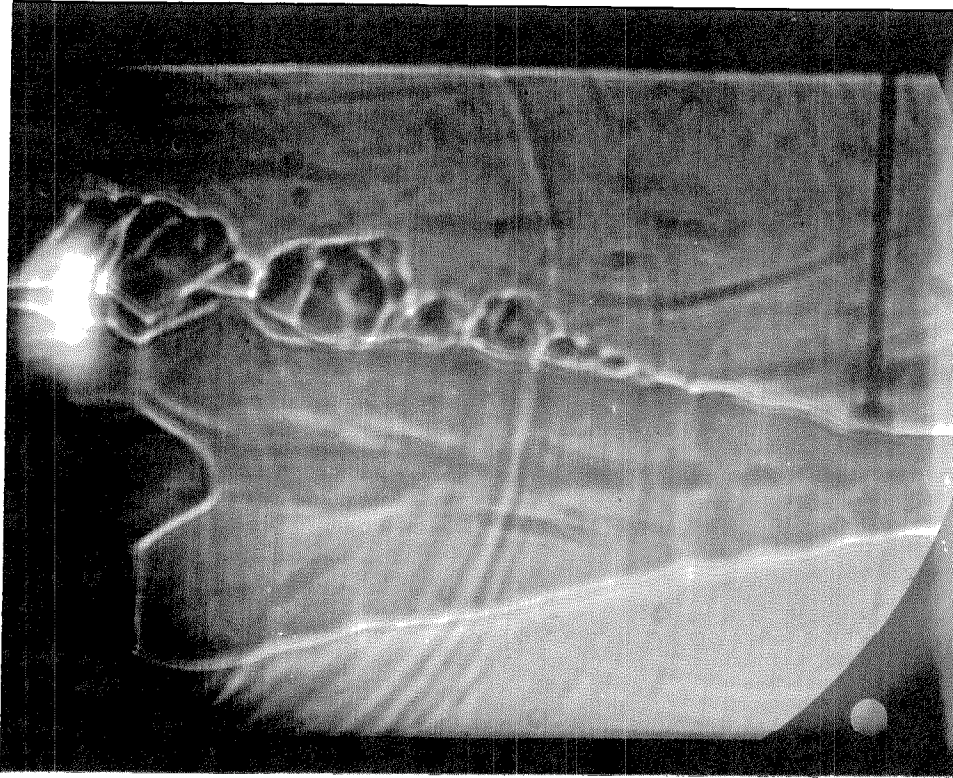


Figure 31

Effect of Turbulent Wake on Flame Front

0.065 in. Diameter Turbulence Source

$U_o = 29.4$ ft/sec

$\phi = 0.87$

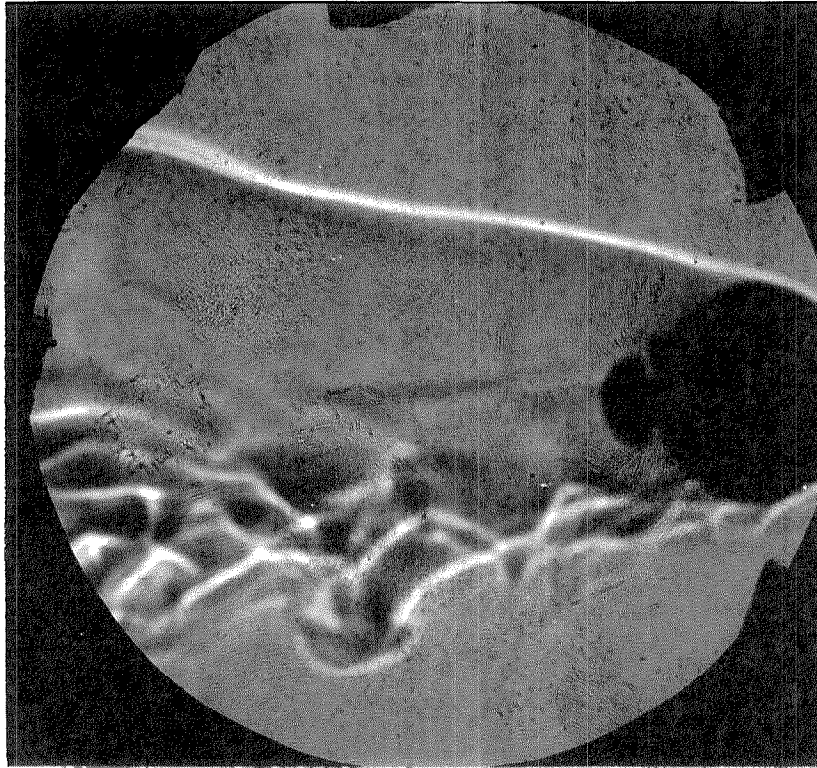


Figure 32

Effect of Large Turbulent Wake on Flame Front
0.095 in. Diameter Rod for Turbulence Source
Located Parallel to Line of Sight Below
and to the Left of the 0.5 in. Diameter
Flame Holder

$U_o = 7.4 \text{ ft/sec}$
 $\phi = 0.64$

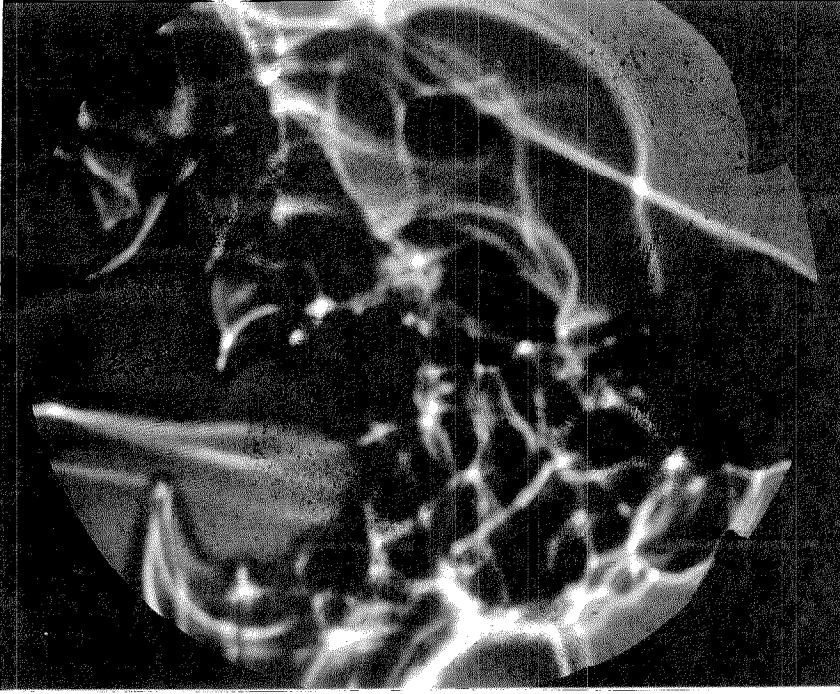


Figure 33

Effect of Large Turbulent Wake on Flame Front
0.095 in. Diameter Rod for Turbulence
Source

$U_o = 7.4 \text{ ft/sec}$
 $\phi = 0.72$